

1 **Synthetic strategies and application of gold-based nanocatalysts for**
2 **nitroaromatics reduction**

3 Lei Qin ^{a,b}, Guangming Zeng ^{a,b,*}, Cui Lai ^{a,b,*}, Danlian Huang ^{a,b}, Chen Zhang ^{a,b}, Min
4 Cheng ^{a,b}, Huan Yi ^{a,b}, Xigui Liu ^{a, b}, Chengyun Zhou ^{a, b}, Weiping Xiong ^{a,b}, Fanglong
5 Huang ^{a,b}, Weicheng Cao ^{a,b}

6 ^a *College of Environmental Science and Engineering, Hunan University, Changsha,*
7 *410082, PR China,*

8 ^b *Key Laboratory of Environmental Biology and Pollution Control, Hunan University,*
9 *Ministry of Education*

* Corresponding author at: College of Environmental Science and Engineering, Hunan University, Changsha, Hunan 410082,

China. E-mail address: zgming@hnu.edu.cn (G.M. Zeng) and laicui@hnu.edu.cn (C.Lai).

10	Contents	
11	1. Introduction	4
12	2. Synthetic strategies for Au nanocatalysts	7
13	2.1. Deposition-precipitation	8
14	2.2. Co-deposition	9
15	2.3. Impregnation	10
16	2.4. Colloid deposition	10
17	2.5. Newly developed methods	12
18	3. Mechanism of catalytic reaction.....	13
19	3.1. Kinetic model	13
20	3.2. Route of reaction and possible mechanism	15
21	4. Reduction of nitroaromatics with free AuNPs: Size-dependent effect.....	19
22	4.1. Extract of biomass stabilized free AuNPs	20
23	4.2. Gel and other ligands stabilized free AuNPs.....	21
24	5. Reduction of nitroaromatics with supported AuNPs: Structure-dependent effect	22
25	5.1. Polymer	23
26	5.2. Oxides for lots of materials	26
27	5.2.1. SiO ₂	26
28	5.2.2. TiO ₂	29
29	5.2.3. Other metal oxides.....	31
30	5.3. Carbon materials.....	34
31	5.3.1. Porous carbon	34
32	5.3.2. Graphene.....	35
33	5.4. Multi-metal alloy or doping.....	36
34	6. Reduction of nitroaromatics with non-spherical AuNPs: Shape-dependent effect	39
35	6.1. Polyhedral Au nanocrystals	39
36	6.2. Irregular Au nanocrystals	39
37	7. Comparison with other metal catalysts.....	41
38	8. Conclusions, future outlook and challenges	42
39		

Abstract

With the increasing requirement of efficient organic transformations on the basic concept of Green Sustainable Chemistry, the development of highly efficient catalytic reaction system is greatly desired. In this case, gold (Au)-based nanocatalysts are promising candidates for catalytic reaction, especially for the reduction of nitroaromatics. They have attracted wide attention and well developed in the application of nitroaromatics reduction because of the unique properties compared with that of other conventional metal-based catalysts. With this respect, this review proposes recent trends in the application of Au nanocatalysts for efficient reduction process of nitroaromatics. Some typical approaches are compared and discussed to guide the synthesis of highly efficient Au nanocatalysts. The mechanism on the use of H₂ and NaBH₄ solution as the source of hydrogen is compared, and that proposed under light irradiation is discussed. The high and unique catalytic activity of some carriers, such as oxides and carbons-based materials, based on different sizes, structures, and shapes of supported Au nanocatalysts for nitroaromatics reduction are described. The catalytic performance of Au combining with other metal nanoparticles by alloy or doping, like multi-metal nanoparticles system, is further discussed. Finally, a short discussion is introduced to compare the catalysis with other metallic nanocatalysts.

Keywords: Au nanocatalysts; Synthesis; Reduction; Nitroaromatics; Metal nanoparticles.

1. Introduction

Metal nanoparticle (NP) catalysts play a dominating role in production of chemicals, polymers, and fuels (Lim 2016, Mitsudome et al. 2015). They are the keys to the environmental protection, like clean-up of effluent gases and degradation of pollutant substance (Wang et al. 2014, Zhao et al. 2016a). Gold (Au), one kind of noble metals, is historically considered as a catalytic inert element until Hutchings and Haruta observed that Au catalysts were highly efficient in chlorination of acetylene and carbon monoxide oxidation at 1980s (Haruta et al. 1989, Hutchings 1985). When subdivided to nanoscale, Au-based catalysts provide incredible reactivity for catalysis, which is hard to be replaced by other metals, especially for the reduction process like oxygen and carbon dioxide reduction, water reduction for hydrogen production, and reduction of nitroaromatics because of its unique properties of localized surface plasmon resonance (LSPR), large surface-to-volume ratio, and electron transfer (Chung et al. 2018, Hutchings and Haruta 2005, Li et al. 2018a, Qin et al. 2018, Wang et al. 2018a). Au nanocatalysts also have been demonstrated to be attractive in industry and environmental protection due to their green and efficient redox properties (Scurrrell 2017). They are widely used and the topic of Au nanostructured catalysts has been augmented exponentially in the last 20 years.

Gold nanoparticles (AuNPs) with small size show excellent catalytic performance for many chemical reactions, especially for the reduction of nitroaromatics in water (Hirakawa et al. 2016, Moghaddam et al. 2017). Some nitroaromatics, such as nitrophenol compounds, organic dyes, etc., are important intermediates in industrial and

agricultural processes (Chen et al. 2015, Cheng et al. 2016b, Cheng et al. 2017, Gong et al. 2009, Hamidouche et al. 2015). However, environment has been suffered from pollution at significant levels because of the high toxicity of these compounds (Cheng et al. 2016a, Huang et al. 2017a, Tang et al. 2014, Xue et al. 2018). The use of nitroaromatics is difficult to forbid, hence, these chemicals are inevitably discharged into the environment (Cheng et al. 2016c, Huang et al. 2016, Rafatullah et al. 2010, Yang et al. 2010). Therefore, **remove and degrade** these compounds to less toxic chemicals **are** very important. In this case, AuNPs exhibit **good** catalytic activity for reduction of nitroaromatics to its **corresponding amines**, because they have the advantages of large surface-to-volume ratio and unique electronic properties (Downing et al. 1997, Kuroda et al. 2009). They stabilize the $6S^2$ electron pairs by combining the size and relativistic effect, thus determining the catalytic property for nitroaromatics reduction because of the high energy and reactivity of 5d electrons (Narayanan and Sakthivel 2011, Pyykko 1988). **Compared with other metal catalysts, AuNPs have two distinct advantages: 1) the catalytic activity is highly and directly related to the particle size that must be nanoscale but not microscale. Besides, the catalytic activity is increased with the decrease of particle size. Thus, the catalytic activity of Au can be well controlled by adjusting the size; 2) The high catalytic performance can be obtained under mild conditions even on low temperature. This is benefit for the reduction under ambient temperature and energy saving.**

Unfortunately, **free AuNPs cannot be recycled** and are easy to aggregate due to the high surface energy, which significantly decreases the catalytic efficiency and

obviously slows the reaction kinetics (Pocklanova et al. 2016, Qin et al. 2017). The surface active sites and interfacial free energy are reduced due to the aggregation, hence weakening the catalytic activity (Varma 2016). In order to solve this problem, great efforts are being devoted to immobilize AuNPs on carriers, such as oxides (Lee et al. 2008, Song and Hensen 2013), carbon-based materials (Tan et al. 2015, Yang et al. 2013), etc., for obtaining effectively stable and highly dispersed Au nanocatalysts, offering more surface active sites, and enhancing the interfacial free energy. Moreover, some strategies tend to investigate the size and structure of AuNPs by using different reducing agent and stabilizer, alloying other metal NPs, and decorating some ligands to form smaller and bimetallic or multi-metallic catalysts (Conte et al. 2009, Fountoulaki et al. 2014, Huang et al. 2017b, Sau et al. 2001). Due to the size effect, synergistic effect, interfacial effect and shape effect between the supports and Au, easily separated, well cycled, and highly efficient Au nanocatalysts can be obtained. Thus, Au nanocatalysts provide promising potential in catalytic reaction.

Some wonderful reviews have been published about nitroaromatics reduction on the basis of Au and other metal NPs (Mitsudome and Kaneda 2013, Pan et al. 2013). For example, Kadam et al. reviewed the different methods for nitroaromatics reduction based on the source of hydrogen (Kadam and Tilve 2015). Aditya et al. reported a comprehensive paper, which mainly focused on the reaction process, mechanism, and catalytic performance of different kinds of catalysts (Aditya et al. 2015). However, none of them have reviewed the nitroaromatics reduction by Au nanocatalysts only. Zaho et al. synthetically reviewed the nitrophenol reduction by Au- and other transition metal

nanoparticles and discussed the difference between them in detail (Zhao et al. 2015). But the synthetic methods for Au nanocatalysts was not mentioned. Furthermore, the investigation of Au nanocatalysts for nitroaromatics reduction has been developed in the past four years, especially for the reduction under light irradiation. Hence, in this review, some typical synthetic approaches for Au nanocatalysts including the traditional and novel methods have been reviewed and discussed to guide the fabrication of highly efficient Au nanocatalysts. The unique catalytic activity of them in reduction of nitroaromatics has been discussed. The kinetic model and route of this reaction are represented to reveal the potential mechanism under different conditions, including the reaction medium and light effect. This review further emphasizes some typical and recent examples of Au nanocatalysts that have achieved high activity and compares the catalytic performance of them. A short discussion is introduced to compare the catalysis with other metallic nanocatalysts. Through this review, the readers will understand the role of Au nanocatalysts in catalytic reaction profoundly. We hope that readers can be inspired by this review and gain more highly efficient Au nanocatalysts, pushing further development of Au catalysts application.

2. Synthetic strategies for Au nanocatalysts

The preparation of colloidal AuNPs has been well described in many researches (Dykman and Khlebtsov 2012, Qin et al. 2017, Zhang et al. 2014a). AuNPs fabricated through Brust-Schiffrin method are primarily used for catalysis because it provides smaller size of AuNPs. The procedure has been well described in our previous works (Fang et al. 2017, Guo et al. 2016, Lai et al. 2015, Lai et al. 2017, Zeng et al. 2017). In

this section, we mainly retrospect some typical synthetic strategies for supported Au nanocatalysts, which are widely applied in the reduction of nitroaromatics. They can be usually divided into five parts: the deposition-precipitation (DP), co-deposition (CP), impregnation (IMP), colloid deposition (CDP), and newly developed methods.

2.1. Deposition-precipitation

DP is one of the earliest strategies for preparation of supported Au nanocatalysts, which was recognized by Haruta and co-workers, who reduced AuNPs on titanium dioxide (TiO₂) firstly (Tsubota et al. 1991). The operation procedure consists in allowing Au salt become Au(OH)₃ by adding alkali, the precipitant, into the Au salt solution to adjust the pH with the range of 6 to 10. After aging for a while, the aforementioned Au solution is adsorbed by the support and the mixture is incubated with properly selected concentration, temperature, stir, and time. Subsequently, the suspension is treated by a series procedure of filtration, washing and drying. The last and most important procedure is the reduction of AuNPs from Au³⁺. Some studies kept it under a flow of H₂, and others made it be calcined in a flow of O₂ or air (Song et al. 2015, Ulrich et al. 2017, Wang et al. 2015a). The calcined Au nanocatalyst provides better performance but some deactivation has been observed due to the increasing particle size when sintering.

The key procedure of this method is the strict control of pH. It can be adjusted by precipitant, which usually uses Na₂CO₃, urea, NaOH, etc. (Torres et al. 2016). DP requires deposition occurs in alkaline condition, so it is applicable in supports which have a point zero charge at a high pH (≥ 6), e.g. TiO₂, ceria (CeO₂), zirconia (ZrO₂),

ferric oxide (Fe_2O_3), aluminum oxide (Al_2O_3), and magnesium dihydroxide (Prati and Martra 1999, Xu et al. 2012b). Other supports, e.g. carbon, silica dioxide (SiO_2), and tungsten trioxide, cannot obtain well dispersed and small size of AuNPs by using this method (Chen et al. 2006). Before reduction step, AuNPs are partially deposited on the supports. Hence, the loading of Au may be incomplete, but much higher than CP method (mentioned as follows) (Khoudiakov et al. 2005). Besides, the most attractive merit of DP is that AuNPs can deposit on supports with any kind of shapes, including powder, honeycomb, bead, or thin film (Torres et al. 2016). AuNPs are mostly deposited on the surface of supports, which contributes to the catalytic performance of Au nanocatalysts.

2.2. Co-deposition

Similar with DP, CP uses an aqueous solution of Au salt. The Au salt is mixed with a corresponding metal salt precursor and stirred under a certain temperature. The precipitant is added to obtain hydroxide or carbonate coprecipitate. After that, the slurry is filtered, washed, and dried. Finally, the precursor is calcined for AuNPs reduction as DP method (Waters et al. 1994). The difference of CP and DP is the mixture of reaction. In this regard, CP also can be called the one-step synthetic method. The Au particles are regularly dispersed and in nanoscale but the particle size may be increased during calcine as the DP method and the size is difficult to control sometimes. This procedure requires the precursor compound of support to become hydroxide or carbonate, which can be deposited with $\text{Au}(\text{OH})_3$ at the step of deposition (Solsona et al. 2009).

2.3. Impregnation

IMP is the simplification of DP and CP. It is unnecessary to adjust the pH, namely, there is no need to add alkali salts as the precipitant (Solsona et al. 2006). When the Au source salts injected into the dried support, after technical filtration, washing and drying in appropriate temperature, the resulting catalysts are further calcined in a flow of O₂ or H₂ (Grisel et al. 2001). IMP is much simpler and usually used to prepare Au nanocatalysts which need certain mechanical strength rather than high content of active component. As a result, it has been widely used in industry. However, the low content of active component is not conducive to catalytic reaction. It is reported that this is commonly related to the size and size distribution. But there are evidences demonstrate that the low activity of MIP is due to the lack of some kind of interaction between AuNPs and support (Lin and Vannice 1991, Lin et al. 1993). Additionally, the pH of Au salts solution is always very low, so this method is not so suitable for some supports which can be dissolved in a strong acidic solution, e.g. Al₂O₃ and magnesium oxide (MgO).

2.4. Colloid deposition

CDP method, also called the immobilization method, is theoretical different with these traditional methods mentioned above. Generally, AuNPs are reduced first by appropriate methods, e.g. Turkevich-Frens and Brust-Schiffrin method, to obtain colloids rather than load on the support through sintering and reduction. Thus, the size can be well controlled by this method. Subsequently, the prepared AuNPs are injected into the support or the support is dipped into the AuNPs solution for incubation a few

214 days until AuNPs are completely adsorbed by support. Resulting catalyst is finally
215 prepared by filtering, washing, and drying. The key procedure lies in the adsorption of
216 AuNPs by support. In this case, the support should have large surface area with strong
217 adsorption ability and can be washed so clean that it would not induce aggregation of
218 AuNPs. With this respect, the adsorption of AuNPs into gel has been well developed.
219 A typical example is the silica gel. Yutaka Tai (Tai et al. 2001) prepared an Au
220 cluster/SiO₂ nanocomposite catalyst by spontaneous wet-gel formation. Results
221 demonstrated that the colloids were penetrated into the gel and were adsorbed only on
222 the surface of the gel due to the reaction between gel and polar solution. The anchoring
223 of AuNPs was because the surrounding thiol molecules of AuNPs had a permanent
224 dipole moment, which induced the dipole interaction. In addition, the particle sizes and
225 size distribution were not changed. On the basis of this mechanism, thermally stable
226 and highly loaded AuNPs/TiO₂-coated SiO₂ aerogels are prepared with the controlled
227 size and loading amount of Au (Tai et al. 2004, Tai and Tajiri 2008).

228 Other supports, e.g. metal-oxide particles (Nutt et al. 2006, Zheng and Stucky 2006),
229 activated carbon (AC) (Biella et al. 2002), mesoporous carbon (MC) (Ma et al. 2013),
230 oxidized mesoporous carbon (OMC), carbon nanotubes (CNTs), and graphite (GR) (Qi
231 et al. 2015) have been well developed for supported Au nanocatalysts synthesis using
232 both weak and strong interactions. In particular, the adsorption way of MC or OMC-
233 supported Au nanocatalysts is that AuNPs with small size are incorporated into the
234 larger size of mesopore channels thus preventing the aggregation of AuNPs. In addition,
235 the stabilizer plays an important role in the size and catalytic performance (Shi et al.

2008, Zhong et al. 2013). Robert group **has** developed a series of experiments about the n-hexanethiolate-stabilized AuNPs catalysts supported by metal oxide. Results showed the size of AuNPs increased during subsequent thermolysis (Almukhlifi and Burns 2015a). The length of n-hexanethiolate and Au content had influences on the catalytic performance of **Au nanocatalysts** (Almukhlifi and Burns 2015b, 2016a). Furthermore, the presence of small amount of sulfate enhanced the catalytic activity owing to an Au-enhanced Mars-van Krevelen mechanism (Almukhlifi and Burns 2016b).

2.5. Newly developed methods

The aforementioned methods for Au nanocatalysts preparation are traditional and mainly applied in some simple supports and the size and size distribution may be difficult to control. In this case, for the controlling of size and size distribution and some relatively complicated supports and structure like polyhedral anatase, Au@oxide yolk@shell nanospheres, some novel methods including polyols reduction (Yang et al. 2013), photo- and electro-deposited method (Nguyen et al. 2016, Wei et al. 2017b), etc., have been well developed. The photo-deposited method are usually proposed by putting the mixture of supports and Au salt under the UV/vis irradiation and using methanol as the sacrificial agent (Maicu et al. 2011). Other photo-deposited method like pulsed laser ablation was also developed (Wei et al. 2017a, Xu et al. 2014). This method is suitable for the preparation of photocatalyst, in which the supports have good photocatalytic activity and AuNPs are easy to deactivate in air when using other methods. **Pulse electrodeposition method is another newly developed method, in which the size and**

dispersion of AuNPs can be easily achieved via changing the electrochemical parameters. The prepared Au nanocatalyst by this method exhibits excellent plasmon-induced photoelectrocatalytic activity (Wu et al. 2015a). Au nanocatalysts synthesized by photo- and electro-deposition only need one-step and do not need the use of surfactant or additive. The catalytic activity of them are improved by making use of the plasmonic effect of AuNPs, which is conducive to the application of Au nanocatalysts in photoelectrocatalysis. But the introduction of light energy or electricity is necessary.

Au@oxide yolk@shell nanospheres provide good catalytic performance because of their low density, high specific surface area, stability, and selectivity. They can propose promising application on selective catalysis by controlling the pore size of the shell accurately. However, this kind of Au nanocatalyst is usually prepared by using etching or template method, which are suitable for single oxide shell. Interestingly, the group of Zhang (Li et al. 2018b) recently has proposed a new strategy for preparation of Au@multi-oxide yolk@shell nanospheres system by integrating redox self-assembly and redox etching process. This simple strategy provides new avenue for facile and clean synthesis of complex noble metal@multi-oxide yolk@shell nanospheres. Although these newly developed methods illustrated here are mainly for photocatalysis or other catalytic processes, they are still instructive for the preparation of highly efficient Au nanocatalyst and guidance of nitroaromatics reduction reaction.

3. Mechanism of catalytic reaction

3.1. Kinetic model

The traditional Langmuir–Hinshelwood (LH) model is usually used in the kinetic

analysis of nitroaromatics reduction by **Au nanocatalysts**. Namely, all of the reactants are absorbed on the surface of AuNPs to react. Kinetic data can be obtained by monitoring the concentrations of nitroaromatics via UV-vis spectroscopy. The subsequent data calculation yields the apparent reaction rate, k_{app} , one of the most important parameters to assess the catalytic property of **Au nanocatalysts**. The analysis of kinetic data has been well described by Wunder et al. (Wunder et al. 2010), who used the reduction of 4-nitrophenol (4-NP) as a model reaction to test the catalytic activity of **Au/platinum (Pt)** NPs (**Fig. 1**). They proposed a series of studies by immobilizing AuNPs on the spherical polyelectrolyte brushes and demonstrated that k_{app} was not only concerned with the total surface of all AuNPs (S), but also the rate-determining step, as well as the adsorption constants of 4-NP and borohydride (k_{4-NP} and k_{BH_4}). Moreover, as k_{app} is strictly proportional to S (Panigrahi et al. 2007, Saha et al. 2009), the relations are well depicted as the following equations (Wunder et al. 2011):

$$\frac{dc_{4-NP}}{dt} = -k_{app} \cdot c_{4-NP} = -k_1 \cdot S \cdot c_{4-NP} \quad (1)$$

$$k_{app} = \frac{k \cdot S \cdot K_{4-NP}^n \cdot c_{4-NP}^{n-1} \cdot K_{BH_4} \cdot c_{BH_4}}{(1 + (K_{4-NP} \cdot c_{4-NP})^n + K_{BH_4} \cdot c_{BH_4})^2} \quad (2)$$

where S is the total surface of all AuNPs, n is the Langmuir–Freundlich exponent and when using the classical Langmuir isotherm, the value of n is 1 (Gu et al. 2014). Another important parameter, which implies the catalytic activity, is the normalized rate constant (k_{nor}). It is associated with the amount of **Au nanocatalyst** and k_{app} , i.e.,

$$k_{nor} = k_{app}/m. \quad (3)$$

With this respect, almost all of the researches demonstrate that Au dependent catalysis of nitroaromatics reduction is well accorded with the pseudo-first-order

kinetics; that is, the logarithm of absorption intensity of 4-NP (A_t) has a good linear correlation with reaction time (t), then k_{app} can be determined from the plot of $\ln(A_t)$ vs t (Que et al. 2015, Ramirez et al. 2017).

$$\ln(A_t/A_0) = -kt \quad (4)$$

Interestingly, there are several evidences proved that the reduction of nitroaromatics by **Au nanocatalysts** may fit the zero-order kinetic model; i.e. the A_t rather than $\ln(A_t)$ varies linearly with t (Gupta et al. 2014, Saha et al. 2009). They believe that this is due to the different rate-determining steps. Gupta et al. (Gupta et al. 2014) presented the six sequential electron transfer had critical role on this rate-limiting step. However, they did not provide any experimental data to support the speculation. While some studies considered that with the excess of both **Au nanocatalysts** and **sodium borohydride (NaBH_4)**, the reaction rate was the pseudo-first-order (Lee et al. 2008, Pozun et al. 2013). In any case, there may be some other factors result in the different kinetic reaction, such as temperature, **supports**, concentration of reactants, etc. This should be further investigated. One relatively clear thing is that the group of Ballauff has demonstrated that the second step, i.e. the reduction of the 4-hydroxylaminophenol is the rate-determining step (Gu et al. 2014). The reduction of the 4-hydroxylaminophenol is involved in the route of reduction reaction, so it will be discussed in section 3.2.

Please insert **Fig. 1**

3.2. Route of reaction and possible mechanism

The reductants type and effect on this reaction has been well introduced by Kadam and Tilve (Kadam and Tilve 2015). Hence, in this part we just discuss the reaction

triggered by H₂ and borohydride. In order to understand the mechanism better, researchers begin paying their attention to the investigation of route of reaction since Haber proposed that there were two probable routes for reduction of nitroaromatics by Au nanocatalysts, which used H₂ as the reductant to attack the nitro group to form corresponding amino group (Fountoulaki et al. 2014, Layek et al. 2012). One is the generally accepted direct route and another is the condensation route. In the direct route, the nitroso compounds are reduced firstly, and then the corresponding hydroxylamine is fast consecutively produced. Finally, the corresponding aniline derivatives are generated in the rate determining step (Fig. 2). The whole process is very fast and relatively simple. While in the condensation route, the azoxy compounds are synthesized after combining one molecule of nitroso compound and hydroxylamine respectively. The corresponding aniline derivatives can be obtained after a series of steps to azo and hydrazo (Fig. 2). Obviously, the condensation route is much more tedious. As the reaction of nitroaromatics reduction by Au nanocatalysts is always fast, some researchers are skeptical about this conclusion. Thus, confirmatory experiment has been proposed based on supported Au nanocatalysts. Corma et al.(Corma et al. 2007) elaborated on the reduction of nitroaromatics by Au/TiO₂ catalyst and perfectly proved this reduction process followed the direct route. However, in these process, the reduction of nitroaromatics was proposed by H₂ as the reductant, the process using NaBH₄ is different.

Please insert **Fig. 2**

Based on the LH model, Layek et al.(Layek et al. 2012) proposed a probable surface

reduction mechanism making use of Nano ActiveTM Magnesium Oxide Plus (NAP)-
Mg–Au(0) catalyst for reduction of nitroaromatics by NaBH₄ (**Fig. 3**). To verify the
reaction pathway, possible intermediates were separately subjected to the reduction
process. Results showed that the direct route including nitrobenzene → nitrosobenzene
→ phenylhydroxylamine → aniline was the most possible route. In addition, the authors
introduced that the possible reduction mechanism laid the foundation for the six
electron transfer process. AuNPs reacted with borohydride ions to form an Au-H
complex firstly. Then, the targets adsorbed on the surface of AuNPs and a hydrogen
transfer occurred. Finally, the nitro group was reduced to amino group. In 2014, Gupta
et al. (Gupta et al. 2014) proposed a six-electron transfer process between NaBH₄ and
nitrophenol compounds, but how did the electron transfer was not reported. Recently, a
paper based on the magnetic Ni-Au/graphene nanocomposites introduced that the
transition metal composited had the ability to catalyze hydrolysis of NaBH₄ (Li et al.
2017). The NaBH₄ reacted with H₂O to form activated hydrogen (H₂) and then the
metal-hydrogen species formed on the surface of catalyst. Finally, these active metal-
hydrogen species attacked 4-NP to reduce it. In conclusion, no matter reducing by H₂
or NaBH₄, the critical step is the attack of –NO₂ by hydrogen. AuNPs play important
role to transfer and promote the attack. Recently, Wang et al.(Wang et al. 2017a)
concluded the same route as Layek et al. for reduction of nitroarenes by SiO₂-supported
Au nanocatalyst. However, different results were proposed by Fountoulaki et al.
(Fountoulaki et al. 2014), in which the nitrosoarene intermediates were skipped
following the routes of nitroarene → aryl hydroxylamine → aniline. In addition,

Noschese et al. (Noschese et al. 2016) found that both the direct and condensation routes were possible on the basis of a nanoporous polymer matrix supported Au nanocatalyst, but the condensation route was preferred when the Au active sites were more accessible.

Please insert **Fig. 3**

Interestingly, when expose to the light, the catalytic mechanism changes. As described by Koklioti et al., (Koklioti et al. 2017) the presence of photoillumination yields an electron-hole pair, and therefore increases the density of active sites on the surface of Au clusters, resulting in enhanced catalytic performance for 4-NP reduction. There are three possible ways can cooperate to the reduction of 4-NP: i) common hydride transfer from Au-H bond both in the absence and presence of light; ii) specific hydride transfer by photoinduced Au-H bond; iii) active hydrogen generated via photoreduction of water (**Fig. 4**). In addition, the photogenerated electrons may also play an important role in the enhancement of catalytic performance. As introduced by a recent paper (Fu et al. 2017), under the exposure of visible light, electrons in the valence band of support were excited to the conduction band (CB), resulting in rapid electron transfer from CB of support to AuNPs. This makes AuNPs store abundant electron. With the continuously increasing of electron density, the Fermi level of them becomes more negative potential, thereby further improving the catalytic activity.

Please insert **Fig. 4**

As we all known, the reduction of nitroaromatics by Au based-nanocatalysts are almost proposed in aqueous medium at ambient temperatures because most of them use

NaBH₄ as the resource of H₂. However, the reaction proposed by other metal nanocatalysts such as nickel (Ni) based-nanocatalysts has been proceed in other medium. For example, Xia et al. (Xia et al. 2016) introduced a carbon black supported nano-Ni catalyst for reduction of 4-NP and compared the catalytic performance of it under different medium. The results showed that the catalyst exhibited higher activity in methanol than that in aqueous solution because the methanol-NaBH₄ reaction system generated much more amount of H₂ than the water-NaBH₄ system. Inspired by this, we also investigated the effect of reaction medium by using methanol and ethanol as the medium and found that the generation of H₂ was very less in these medium. We speculate this is because NaBH₄ is less soluble in methanol and ethanol. In addition, the nitrophenol reduction in most cases is proceeded by nitrophenolate ion which is mainly prompted in aqueous medium. This also maybe the reason that most researchers have chosen the reaction in aqueous medium. Thus, the illustrated studies for reduction by Au nanocatalysts in this review are almost proposed using NaBH₄ as the reductant.

4. Reduction of nitroaromatics with free AuNPs: Size-dependent effect

Free AuNPs for reduction of nitroaromatics have been investigated for many years. The study of catalysis by free AuNPs mainly focuses on the influence of size and synthetic method. Generally, the catalytic activity is enhanced for smaller size of AuNPs. But the catalytic activity is also related to the surface area and mass of particles. For example, Sau et al. (Sau et al. 2001) investigated the effect of particle size with the range of 10-46 nm under the same surface area and found that the catalytic rate of eosin reduction did not increase proportionately with the increase of size. It decreased first in

the size range of 10-15 nm and then increased with the size over 15 nm. Thus, we discussed the catalytic activity of free AuNPs by the synthetic methods and stated the size effect systematically.

4.1. Extract of biomass stabilized free AuNPs

Bioreduction of metal ions in organism, such as plants, fungi, and bacteria is regarded as an eco-friendly, low cost, and highly efficient way and is important for biomedical application. Plants reduced AuNPs are mostly used in sensors, while Sharma et al. (Sharma et al. 2007) firstly reported plant-mediated AuNPs for directly reducing 4-NP. Unlike other biological methods, the synthesis of AuNPs by the stem extract of *Breynia rhamnoides* is very fast and the size of that can be tuned (Gangula et al. 2011). Recent researches for bioreduction of AuNPs used in catalysis primarily lie in the extract or some parts of them, including dextrose (Badwaik et al. 2011), mycelia (Narayanan and Sakthivel 2011), protein (Guria et al. 2016, Shi et al. 2015), and membrane-bound peptides (Srivastava et al. 2013) etc. Most of the results proved that the catalytic rates increased with the size decrease (Badwaik et al. 2011, Zhu et al. 2016). It is noteworthy that the size and shape controlled synthesis of AuNPs is always achieved a seed mediated grown approach by using some chemical agents. But a research reported by Das et al. (Das et al. 2012) has introduced a simple one-pot green method for biosynthesis of AuNPs and obtains super high catalytic rate for 4-NP reduction with the range of 8.6×10^4 – 2.6×10^6 min⁻¹ by controlling the size and shape. The catalytic rate it achieved is much higher than the other methods (**Table 1**). Particularly, the increasing

catalytic rate can be induced by the decrease of the particle size which could be obtained by adjusting the H₂AuCl₄–extract ratio. Except the size and biomass, the concentration of AuNPs play an important role in catalytic performance. As illustrated by Qu et al. (Shen et al. 2017b), the reaction rate constant was linearly related to the concentration of AuNPs, which resulted in an increase rate from 0.59 min⁻¹ to 1.51 min⁻¹ with the increasing AuNPs concentration of 1.46×10^{-6} to 17.47×10^{-6} mmol.

4.2. Gel and other ligands stabilized free AuNPs

Hydrogels, with tunable structure, are excellent carrier for easy aggregated nanoparticles, especially AuNPs (Kong et al. 2016). The obtained AuNPs-hydrogel nanocomposites have unique property of both metal NPs and hydrogels, which are appealing in terms of green catalysis (Wang et al. 2017c). For example, Zinchenko et al. (Zinchenko et al. 2014) prepared well dispersed and spherical AuNPs with small size of 2-3 nm by injecting the Au precursor into a DNA hydrogel, which allowed for the reduction of H₂AuCl₄. The DNA hybrid hydrogel containing AuNPs provided highly catalytic activity in the reduction of 4-NP to 4-aminophenol (4-AP) with k_{app} of 0.09 min⁻¹. Some biocompatible molecules such as chitosan can be prepared as hydrogel. However, AuNPs are difficult to reduce by this system. Hence, an *in-situ* photoreduction method for producing AuNPs in chitosan-Au^{III} hydrogel system was reported (Wu et al. 2015b). In particular, this strategy had good catalytic performance for reduction of 4-NP to 4-AP with following a pseudo-first-order kinetics.

Cetyltrimethylammonium bromide (CTAB), a well-known surfactant, can be used as

a stabilizer for AuNPs synthesis (Li et al. 2014). CTAB stabilized AuNPs were successfully fabricated for reduction of 4-NP and demonstrated an intermediate size (13 nm) of AuNPs exhibited highest reaction rate, which was 60 times higher than the biggest one (56 nm) (Fenger et al. 2012). Generally, smaller AuNPs propose higher catalytic performance, while the intermediate size of AuNPs are more active than the seeds AuNPs (Nigra et al. 2013). This might be due to the convergence of increasing surface area of AuNPs versus the size of molecule and charge transfer during the reduction process. Besides, seeds AuNPs were too small to efficiently absorb 4-NP. The adsorption process of nitroaromatics was accompanied by a significant charge-transfer from the surface of AuNPs to the N-atom of nitroaromatics. Thus, the charge-transfer played very important role in reduction of nitroaromatics by Au nanocatalysts. The mechanism of this process needs to be further investigated in the future. In conclusion, reducing AuNPs by biomass is fast and green. The size of them can be controllably varied (Gangula et al. 2011).

Please insert **Table 1**

5. Reduction of nitroaromatics with supported AuNPs: Structure-dependent effect

Easy aggregation of free AuNPs results in much loss of catalytic activity, so researchers tend to anchor them on the carrier to retain the catalytic activity and recyclability of AuNPs. The supports, including polymer, oxide, carbon, as well as the combination of them, have been well developed to anchor AuNPs with good dispersion, large loading amount, and narrow size distribution. In this part, we discuss some critical and new studies developed recently, concerning different carrier supported Au

nanocatalysts (Table 2-5).

5.1. Polymer

The research on polymer supported AuNPs mainly follows three directions: i) different shapes which provide different active sites; ii) different kinds of polymers which offer different ligands or functional group; iii) different synthetic routes of supported Au nanocatalysts which achieve several sizes of AuNPs. Different shapes of polymer, e.g. dendrimer, brushes, beads, micelles, nanotubes, flowers, and stars are used for synthesis of supported Au nanocatalysts (Table 2). In the early years, most of these structures preferred to make AuNPs encapsulate into the polymer networks, rarely on outside, which restricted the contact between nitroaromatics and AuNPs in some degree (Wang et al. 2007). Interestingly, Haruta and co-workers (Kuroda et al. 2009) developed a deposition reduction method that directly deposited AuNPs on the surface of poly(methyl methacrylate) (PMMA) beads with 6.9 nm average size of AuNPs. This reported Au nanocatalysts provided a highest rate constant of $0.432\text{--}0.474\text{ min}^{-1}$ among ever reported Au/polymers catalysts. In addition, this report proposed the importance of moderate interaction between polymer supports and AuNPs, which indicates the structure-dependent effect. Hence, many research groups have concentrated their attention on deposition sites of AuNPs and structure of polymers. For example, Qiu et al. (Qiu et al. 2012) successfully prepared an efficient electrocatalyst, polypyrrole nanotube (PPyNTs)-supported AuNPs, for catalytic reduction of 4-NP. Hu et al. (Hu et al. 2017) carried out a hyperstar polymer–Au₂₅(SR)₁₈ nanocomposite for 4-NP

reduction using hyperbranched copolymers as macroinitiators to polymerize the polymer. This obtained hyperstar-Au₂₅(SR)₁₈ catalyst showed great stability and convenient recovery and could be reused without losing any catalytic efficiency.

Please insert **Table 2**

Some polymers, such as poly(amidoamine), poly(propyleneimine), poly(2-(dimethylamino) ethyl methacrylate) (PDMAEMA), and poly(glycidyl methacrylate), etc., are well reported for reducing and stabilizing AuNPs. Most interests concern the catalytic performance of different polymers supported AuNPs, but speculation is starting concerning the reactions between AuNPs and the ligands of polymer. For instance, Zeng et al. (Zeng et al. 2013) developed a polydopamine (PDA)-encapsulated magnetic microspheres supported **Au nanocatalyst** for catalytic reduction of nitrobenzene on the basis of interaction between PDA and AuNPs. The strong combination of AuNPs and –NH₂ of PDA made AuNPs be well reduced and dispersed. It is reported that some ligands such as –SH, –NH₂, **–OH**, etc., have an effect on the properties of AuNPs surface, thus affecting the available free active sites (Ansar and Kitchens 2016, Menuel et al. 2016). In addition, the catalytic performance is significantly related to the loading amount of AuNPs. Chen group demonstrated a raspberry-like polymer composite sub-microspheres with tunable AuNPs coverage for 4-NP reduction (Liu et al. 2013). The results indicated this model reaction followed the pseudo-first-order reaction kinetics, but the study of kinetics was probably oversimplified. Therefore, they further developed this mechanism and investigated the effects of many factors (**Fig. 5**) (Li and Chen 2013).

Please insert **Fig. 5**

Deposition of AuNPs on polymer is important for synthesizing well dispersed **Au nanocatalysts**. There are two routes for depositing AuNPs on polymer, the direct one and indirect one. The two routes are all based on the formation of polymer supported core-shell structure or brushes. The direct one deposits AuNPs on polymer carrier using NaBH_4 or other weak reducing agent. The ligands or functional groups of polymer molecules play very important role in the formation of well-dispersed AuNPs by electrostatic conjunction of the negatively charged AuCl_4^- or positively charged Au(en)_2^{3+} . Thus the Au precursor salts should be chosen selectively. For example, Chen et al.(Chen et al. 2014a) reported a smart hybrid system that AuNPs were absorbed by $\text{SiO}_2@\text{PDMAEMA}$ carrier and reduced by NaBH_4 . Recently, polystyrene/polyaniline/Au (PS/PANI/Au) composites were fabricated based on the electrostatic attraction between positively charged Au(en)_2^{3+} and sulfonated PS particles (Sun et al. 2017). The sulfonated PS particles can absorb more Au(en)_2^{3+} , hence enhancing the amount of loaded AuNPs and exhibiting excellent catalytic performance with k_{app} of 3.5196 min^{-1} . Another way of depositing AuNPs on the carrier is AuNPs are prepared firstly by Frens or Brust methods, the definite sizes of AuNPs are absorbed by some ligands such as $-\text{SH}$ and $-\text{NH}_2$ subsequently (Liu et al. 2013). This route provides tunable loading amount of AuNPs by changing the pH of solution and concentration of polymer and AuNPs. In addition, the catalytic performance can be adjusted by using different size of AuNPs, which opens a new sight in reduction of nitroaromatics by **Au nanocatalysts**.

5.2. Oxides for lots of materials

5.2.1. SiO₂

SiO₂, a kind of very stable porous material, has been demonstrated as an ideal nonmetallic oxide support for encapsulation of metal NPs due to the confinement effect, offered by their unique properties of mesoporous channels structure, good thermal, and chemical stability (Xie et al. 2015, Zhao et al. 2016b). The way of encapsulated AuNPs in SiO₂ for nitroaromatics reduction can be divided into three channels: i) AuNPs are confined by SiO₂ to form yolk-shell or core-shell structure **Au nanocatalyst**, where SiO₂ is a microsphere; ii) AuNPs are deposited on the inside or outside the surface of SiO₂ nanotubes (SNTs); iii) AuNPs are embedded on the surface of SiO₂ microsphere (**Fig. 6**).

Please insert **Fig. 6**

SiO₂ is always formed by a sol-gel process using tetraethyl orthosilicate (TEOS) as silica source. This procedure can be used in synthesizing **Au@SiO₂** yolk-shell or core-shell structure. With this respect, Lee et al. (Lee et al. 2008) introduced a nanoreactor framework for 4-NP reduction using Au@SiO₂ yolk-shell catalyst. The prefabricated-AuNPs were firstly coated by the shell thickness of SiO₂ through TEOS undergoing hydrolysis. Then the Au cores were selectively etched by different concentration of KCN, which provided different sizes of AuNPs. Thus the rate constants varied as the size of Au core changes. This designed framework was easily separated and dispersed and served as an efficient platform for nitroaromatics reduction. Different with this

strategy, Huang et al. (Huang et al. 2009) reported a similar strategy confining AuNPs in SiO₂ shell, but the etched one was SiO₂ rather than Au core. In this case, each sphere only contained one AuNP. AuNP presented anywhere inside the hollow zirconia sphere, which allowed 4-NP access the active sites of AuNPs easily, thus further enhancing the catalytic performance. Similar with this design, a new core-shell Au@resorcinol-formaldehyde nanosphere based on multiple Au cores have been reported by Chen et al. (Chen et al. 2014b) This catalyst exhibited uniform pore size (2.5 nm) of SiO₂ hollow nanospheres and good catalytic performance for 4-NP reduction with a reaction rate constant 0.08 min⁻¹. The conversion percentage retained 94% after five cycles.

SNTs, providing a high surface area to volume ratio, are deemed as potentially good candidates for Au nanocatalyst supports. The deposited AuNPs onto the inside surface of SNTs are usually dispersed within the mesopore channels (Zhang et al. 2011b). Therefore, the pore diameter of SNTs should be big enough to accommodate encapsulated AuNPs and transit the reactant molecules. In addition, the loading amount of AuNPs has a great impact on the catalytic performance. A paper reported recently demonstrated that higher of the catalyst loading, the reaction time was faster (Miah et al. 2017). In this case, The k_{app} increased from 0.2187 to 2.587 min⁻¹ with the increase of Au loading from 0.033 to 0.167 g L⁻¹ (Miah et al. 2017). Except for loading amount, other factors such as interaction between Au and supports, sites where AuNPs located, as well as reduction method are needed to further investigate (Xing et al. 2017). As shown in **Fig. 7**, two different synthetic methods of SiO₂-confined Au nanocatalyst are proposed using calcine and grind, respectively. The calcined AuCS catalyst has much

bigger size of AuNPs than the ground one (AuAS), thus results in lower catalytic performance for 4-NP and methylene blue (MB) reduction. Additionally, the strong interaction between Au and support and well dispersed Au in AuAS are responsible for highly active in catalytic reduction. By limiting AuNPs in the shell or tubes, the recyclability can be obviously enhanced.

Please insert **Fig. 7**

Deposition AuNPs onto the outside of CNTs mainly uses the strong interaction between AuNPs and some ligands, such as $-SH$ and $-NH_2$ (Jan et al. 2011). For example, Lin et al. (Lin et al. 2012) prepared an amino groups-functionalized CNTs supported Au nanocatalyst for 4-NP reduction. Amino groups were served as active sites to host more AuNPs. Different with the deposition AuNPs onto inside or outside of the SiO_2 support, Cao et al. (Cao et al. 2016) carried out raspberry-like Au/ SiO_2 nanocomposite particles, in which AuNPs were half-embedded in the porous SiO_2 , towards reduction of 4-NP (**Fig. 8**). This structure not only offered a good morphological stability, but displayed a good catalytic activity and recycling performance, which remained 95% conversion of 4-NP after five cycles. Most importantly, hydrazinium hydrate with two amino groups was used to reduce $HAuCl_4$ and the organic ligands were removed through heating.

Please insert **Fig. 8**

Please insert **Table 3**

5.2.2. TiO₂

Embedding AuNPs on metal oxide supports is an efficient way to immobilize AuNPs, which shows high activity and efficiency for nitroaromatics reduction. Metal oxides-supported Au nanocatalysts have gained increasing scientific interest because of the high activity to a variety of chemical reactions as heterogeneous catalysts (Sinatra et al. 2015, Zhou et al. 2018b). The nature of oxide supports plays an important role in the catalytic properties of supported Au nanocatalyst. It may limit the stabilization, activity, and catalytic efficiency because of the metal-support interface (Boronat and Corma 2010). Thus, the interaction between AuNPs and supports should be considered cautiously in order to maximize the synergetic effects.

Although Au nanocatalysts have an efficient catalytic activity for nitroaromatics reduction, most of them do not have the ability of chemoselective reduction. It has been reported that TiO₂ supported Au nanocatalysts have unique behavior for chemoselective reduction of nitroaromatics (Corma and Serna 2006, Tamiolakis et al. 2013). This is because the cooperative effect between Au and TiO₂ makes many very specific adsorption sites present at the boundary between Au and TiO₂ (Lai et al. 2016). During adsorption, H₂ is dissociated on Au and nitroaromatics are adsorbed selectively on the catalysts via nitro groups only, thus allows highly selective reduction (Boronat et al. 2007). The particle size of AuNPs plays a dominant role in determining the catalytic activity for nitroaromatics reduction (Wain 2013). However, different synthetic methods of supported Au nanocatalysts have a great influence on the size of AuNPs. In order to obtain highly active TiO₂-AuNPs catalyst, Damato et al. (Damato et al. 2013)

introduced a two-step polyol approach to prepare size-controlled TiO₂-AuNPs catalyst through step-by-step reduction. This strategy successfully reduced different size of AuNPs about 12, 20, and 25 nm and obviously increased in catalytic activity.

Studies have reported that the substrate defects of TiO₂ could stabilize AuNPs (Chen and Goodman 2006, Yang et al. 2008). Furthermore, AuNPs prefer to nucleate at the surface defects, especially step edges and oxygen vacancies. Significantly, under appropriate conditions, defect sites on the surface of TiO₂ can be produced (Barrett et al. 2016). Hence, TiO₂ is well developed for stabilizing AuNPs and improving the catalytic activity. In this case, Wang et al. (Wang et al. 2016) introduced an efficient strategy for fabricating highly selective Au nanocatalyst in reduction of nitroaromatics by positioning AuNPs on the edge/corner sites of TiO₂ (Fig. 9). Results showed that AuNPs loaded on the edge/corner sites considerably enhanced the catalytic activities. The catalytic activities were much higher than the conventional Au-TiO₂ catalysts. Although the selectivity and activity are enhanced by TiO₂ supported Au nanocatalyst, the yields of desired anilines are still low and needed to improve. In very recent, they further proposed that the conversion of nitroarenes could be as high as 99.5% when using Sn decorate the Au/TiO₂ catalyst (Wang et al. 2018b). This research illustrated that the Sn–O–Ti linkage promoted the formation of oxygen vacancies on TiO₂, which resulted in the high activity and selectivity for metal catalysts (Fig. 10). In addition, AuNPs were necessary for the formation of anilines because the AuNPs/support interface could only reduce nitrosobenzene from nitrobenzene. This strategy theoretically reveals the peculiarity of hydrogenation of nitrobenzene on the Sn-O-Ti

interface and may open the door to highly selective hydrogenation of biomass.

Please insert **Fig. 9**

Please insert **Fig. 10**

5.2.3. Other metal oxides

Other metal oxides, such as MgO (Layek et al. 2012), Al₂O₃ (Shimizu et al. 2009), and Fe₃O₄ (Ge et al. 2008), have been well used as supports for stabilizing AuNPs to prevent aggregation. Most of them have a role in stabilizing free AuNPs and have a synergistic effect with AuNPs for providing more active sites (Chaplin et al. 2006, Han et al. 2017, Song et al. 2015). Nevertheless, the recyclability of AuNPs from many supports-containing systems is very difficult and also hinders the monitoring process of catalytic reaction by UV-vis spectrophotometer because of the presence of suspended NPs in reaction solution (Lee et al. 2010). As a consequence, pursuing for efficient separation technique to improve the efficiency is very important. Interestingly, as a magnetic metal oxide, Fe₃O₄ has the properties of high-surface-area and accessibility, thereby possessing the advantages of being magnetically recoverable and low-cost (Chang and Chen 2006, Long et al. 2011, Xu et al. 2012a, Yu et al. 2005). In this manner, Chen et al. (Chang and Chen 2009) fabricated a novel magnetically recoverable Au nanocatalyst for 4-NP reduction by adsorption-reduction of Au³⁺ ions on chitosan-coated Fe₃O₄. Results showed that the catalyst was well separated and did not need either solvent swelling before or catalyst filtration after the reaction.

Different heterostructures of AuNPs-Fe₃O₄ exhibit different catalytic activity toward

nitroaromatics reduction. For instance, the flower- and dumbbell-like AuNPs-Fe₃O₄ heterostructures were prepared (Lin and Doong 2017). They both exhibited bifunctional properties with excellent catalytic activity and high magnetization. However, the dumbbell-like heterostructure suggested much more obvious catalytic performance than the flower-like heterostructure with the pseudo-first-order rate constants of 0.63-0.72 min⁻¹. Substantially, the catalytic activity can be further enhanced using AuNPs-Fe₃O₄ heterostructures. Indeed, a paper reported by Chen et al. (Zheng et al. 2013) has well demonstrated this. Generally, Fe₃O₄ is used as magnetic core, which is coated with SiO₂. AuNPs are loaded on the Fe₃O₄-SiO₂ magnetic nanospheres through Sn²⁺ linkage and reduction (**Fig. 11**). In the case of this design, the catalytic performance is improved with a rate constant of 0.85 min⁻¹. Additionally, it provides convenient magnetic separation and good reusability with a stable conversion of 91% after six cycles.

Please insert **Fig. 11**

AuNPs have attracted wide attention and have been widely used in photocatalytic field, especially in the oxidation reaction, because of its SPR property, which provides strong absorption capacity of visible light (Si et al. 2016, Yang et al. 2015, Yang et al. 2014b). When combining with some semiconductors, the catalytic activity of the catalysts can be changed (Yang et al. 2016b, Zhang et al. 2018). Thus, some reports investigated the reduction of nitroaromatics by Au nanocatalysts under light illumination and compared the catalytic activity in the presence and absence of light. For example, Liu et al. prepared an Au-loaded Na₂Ta₂O₆ nanocomposite photocatalyst for 4-NP reduction and prepared the catalytic activity in the dark and under visible and solar light

irradiation (Liu et al. 2017b) (**Fig. 12**). In the dark, AuNPs only acted as an
electron donor and provided active sites for the reaction. While under visible light
irradiation, the strong SPR of AuNPs excited electrons, more excess activated electrons
were produced, which promoted the catalytic performance. Different with the reaction
process under visible light irradiation, the $\text{Na}_2\text{Ta}_2\text{O}_6$ was easily excited and generated
plenty of free electrons under UV-light irradiation. These electrons then transferred
from the CB of $\text{Na}_2\text{Ta}_2\text{O}_6$ to the surface of AuNPs, which decreased the recombination
rate of charge carriers, the catalysis was further enhanced. Thus, under the irradiation
of solar light, the SPR promotion and charge transfer promotion were responsible for
the high catalytic activity and the catalytic activity was 2.35 times higher than in the
dark. This design also showed good stability and reusability. Similar with this
investigation, other Au-based nanophotocatalysts like silica@apatite@Au composites
(Chen et al. 2018), apatite@Au composite nanosheet spheres (Wang et al. 2018c), and
 $\text{TiO}_2/\text{Au}/\text{CNTs}$ catalyst (Xiang et al. 2014) have been developed for nitroaromatics
reduction under light irradiation. Thus, the catalytic activity for nitroaromatics
reduction can be improved by combining the AuNPs and some semiconductors.
However, not all of the semiconductors have this function. The band potential of
semiconductors should be matched with the Fermi energy of AuNPs, namely the CB of
semiconductors should be higher in energy than the Fermi energy of AuNPs, making
the direct transfer of electrons from semiconductors to AuNPs. More works would be
proposed in the future.

Please insert **Fig. 12**

5.3. Carbon materials

5.3.1. Porous carbon

Carbon-based materials are well known as promising candidates for Au catalytic carriers owing to the characteristic properties of high specific surface area, wonderful mechanical stability, and unique electrical property (Huang et al. 2017b, Yi et al. 2018, Zhang et al. 2016). Carbon-based materials with tailored pore sizes can encapsulate AuNPs inside its pores and leave enough space for reactant passing. Thereby AuNPs are highly dispersed in porous carbon and the porous carbon-encapsulated Au nanocatalysts provide high efficient catalysis for nitroaromatics reduction with good recyclability (Guo and Suslick 2012). MC has been done to disperse AuNPs on it to prevent aggregation and improve the catalytic activity (Wang et al. 2013). AuNPs occupy both the adjacent pore walls and pore channels, but do not penetrate the walls (Wang et al. 2015b). In addition, MC can serve as both carrier and adsorbent for stabilizing AuNPs and adsorbing reactants, respectively. MC with some electron withdrawing groups, such as -COOH and C=O groups, promotes the catch of 4-NP, which exhibits high efficiency to remove 4-NP (Guo et al. 2016).

One of the advantages of carbon carriers is the electron-rich ability (Liang et al. 2017, Zhang et al. 2011a). When linked with AuNPs, the synergistic effect between carbon and Au makes excellent catalytic activity for nitroaromatics reduction. The large surface area of carbon nanomaterials possess high absorption of organic compounds via π - π stacking interactions, hence increasing the opportunity to access nitroaromatics and

AuNPs (Geim 2009, Wu et al. 2017). In this case, a electrospun carbon nanofibers (CNFs) supported Au core-shell catalyst is fabricated for 4-NP reduction (Zhang et al. 2013). Nitric acid, hydrochloric acid and SnCl₂ treated CNFs with rich -OH can reduce and form small size of AuNPs. More 4-NP is absorbed on catalyst through π - π stacking interactions. The electron transfer between CNFs and AuNPs obviously facilitates the uptake of electrons by 4-NP molecules, further improving the catalytic efficiency. It could also be easily recycled for reuse. Distinct from CNFs loaded Au nanocatalyst, AC expresses surface oxygen-containing functionalities, which act as AuNPs anchoring sites, promote the reduction of AuNPs, lower hydrophobicity of Au nanocatalyst and enhance catalyst accessibility during synthesis (Cárdenas-Lizana et al. 2015, Rodríguez-Reinoso 1998). The ultimate goal is to obtain highly efficient Au-based nanocatalyst for nitroaromatics reduction. Nevertheless, the size of AuNPs is needed to decrease in some case.

5.3.2. Graphene

GR, consisting of single-layer and sp²-hybridized carbon lattice with excellent electrical, thermal, and mechanical properties, has been extensively employed as a promising support for Au nanocatalysts (Deng et al. 2013, Liu et al. 2015, Novoselov et al. 2004, Yang et al. 2016a, Zhang et al. 2015). GR as a support for the Au nanocatalysts can improve the conductivity, provide more active sites, and exhibit synergistic effect between AuNPs and GR, which promote the absorption of targets via π - π stacking interaction (Liu et al. 2015, Ying et al. 2017). The catalytic efficiency can

be further improved. For example, a cylindrical piece of AuNPs/GR hydrogel has been synthesized using DP method and illustrates excellent catalytic performance for 4-NP reduction, which is about 14 times larger than the PMMA supported AuNPs mentioned above (Li et al. 2012). The details of these results are shown in **Table 4**. In recent, the development tendency of GR-supported **Au nanocatalysts** is diversification and high efficiency. Maji and Jana (Maji and Jana 2017) synthesized a two-dimensional GR and mSiO₂ supported AuNPs (RGS@AuNPs hybrid) for simultaneous reduction of 4-NP and photo-degradation of MB dye. Graphitic carbon nitride (g-C₃N₄), a sustainable and environmentally friendly metal-free semiconductor which possessing a GR-like two dimensional crystalline structure, is regarded as innovative photocatalytic material (Jiang et al. 2017, Qiu et al. 2018, Vidyasagar et al. 2018, Wang et al. 2017b, Zheng et al. 2016, Zhou et al. 2018a). There are a few researches mentioned it had highly contribution to nitroaromatics reduction, while a recent paper reported the Au/g-C₃N₄ concerted contact system was highly efficient for reduction of 4-NP to 4-AP (Fu et al. 2017). Furthermore, under visible light irradiation, the catalytic efficient was largely enhanced owing to the charge-transfer effect induced by strong interaction between AuNPs and g-C₃N₄.

Please insert **Table 4**

5.4. Multi-metal alloy or doping

Another important typical design for the application on nitroaromatic reduction by Au-based nanocatalysts is in conjunction with other metal NPs e.g. **Pt, silver (Ag), Ni, and palladium (Pd)**, which all have wonderful catalytic performance for chemical

reactions (Gong 2012, He et al. 2017). It is reported that AuNPs alloy or combine with other transition metals to form multi-metal NPs can potentially lead to higher catalytic activity as compared to monometallic NPs (Zhang et al. 2014b). Hammer–Nørskov model identifies that the synergistic effect induced by multi-metal NPs catalysis is mainly due to the d-band of metal surface, which is the controlling factor in chemisorption strength (Pozun et al. 2013). Introduction of another metal NPs results in geometric and electronic effects with structure changes (Tuo et al. 2015). With this respect, many wonderful reports have been published for nitroaromatics reduction by Au-based multi-metal NPs.

AuNPs served as core or shell combine with Ni (Le et al. 2014), Pd (Qian et al. 2014), and Ag (Jayabal and Ramaraj 2014) to form dandelion- and volcano-like structures for highly efficient reduction of nitroaromatics. The bimetallic structure effects are responsible for providing more active sites and exhibiting maximum catalytic activity (Pretzer et al. 2016). Furthermore, the catalytic activity is improved not only by a multi-metallic system, but also by making porous structures (Sahoo et al. 2015). Interestingly, in order to improve the catalytic performance of mono-AuNPs, Godfrey et al. (Godfrey et al. 2017) prepared an Au@Ag@Au (core@shell@shell) structure using the sequential citrate reduction technique. This structure provided a second Au–Ag interface. The extended X-ray absorption fine structure analysis suggested that this structure exhibited an increased proportion of bimetallic interactions and indicated higher catalytic activity than the Au@Ag structure.

The new trend of multi-metal NPs-based catalysts towards nitroaromatics reduction

lies upon loading multi-metal NPs on other supports mentioned above, such as metal oxide and carbon materials. The metal oxide used as carrier mainly have TiO_2 with corner or edges effect to improve the chemoselectivity and Fe_3O_4 with excellent magnetism to separate easily (Boronat and Corma 2010). Particularly, Shen et al. (Shen et al. 2017a) synthesized multifunctional $\text{Fe}_3\text{O}_4@\text{TiO}_2@\text{Ag-Au}$ microspheres by incorporating Au-Ag bimetallic nanostructures onto the $\text{Fe}_3\text{O}_4@\text{TiO}_2$ microspheres, which significantly increased the ‘hot spot’ effect, thereby offering stronger electromagnetic field enhancements (**Fig. 13**).

Please insert **Fig. 13**

Benefiting from the high conductivity and tremendous surface area, GO is widely used as carrier for multi-metal NPs based catalyst. The connection between GO and substrate molecules relies on non-covalent bonding interactions such as hydrogen bonding, hydrophobic π - π stacking, and electrostatic interactions (Rout et al. 2017). GO can reduce metal precursors to form a stable suspension of metal NPs/GO without any reducing agent or surfactant (He et al. 2014). Depending on the design of Au-Pt NPs/GO structure, the catalytic activity for 4-NP reduction is significantly enhanced with k_{app} of 0.228 min^{-1} , which is about 12-fold and 5-fold higher than the value of homemade AuNPs (0.018 min^{-1}) and commercial Pt black (0.042 min^{-1}) (Lv et al. 2015). Moreover, the electron-enhanced effect of RGO support and strong synergistic effect between noble metal NPs play a significant role in long-life stability and excellent catalytic performance (Li et al. 2017). Recently, our team has reported a Pd/Au bimetallic NPs-loaded g- C_3N_4 nanosheet for highly efficient catalytic reduction of 4-

NP. The average diameter around 8 nm of Pd/Au NPs are homogeneously dispersed on the surface of support, which proposed special p-bonded planar structure and large surface area (Fang et al. 2017). The comparison of different parameters of Au-based multi-metal NPs for nitroaromatics reduction is shown in **Table 5**.

Please insert **Table 5**

6. Reduction of nitroaromatics with non-spherical AuNPs: Shape-dependent effect

6.1. Polyhedral Au nanocrystals

The catalytic efficiency of **Au nanocatalysts** not only depends on the particle structure and size, but also on the shape (Cao et al. 2001, Nehl and Hafner 2008). Different shapes of AuNPs have diverse configuration, which provide various active sites, thus have a great impact on the catalytic activity. In early, most of studies concentrated on the synthetic method of different shapes of AuNPs (Rashid and Mandal 2008). Conveniently, Premkumar et al. (Premkumar et al. 2011) fabricated different shapes of polyhedral AuNPs in high yield and investigated the effect on catalytic performance for shape distribution. Differently, a seed-mediated growth approach was employed by Chiu et al. (Chiu et al. 2012) to synthesize cubic, octahedral, and rhombic dodecahedral AuNCs. With this respect, they compared the catalytic activity toward NaBH₄ reduction of 4-NP and found that rhombic dodecahedral AuNCs showed the highest reduction rate.

6.2. Irregular Au nanocrystals

Irregular AuNCs such as rods, flowers, cages, boxes, and stars have been introduced for reduction of nitroaromatics (**Fig. 14**). Nanorods with high surface area of hollow structures show enhanced optical sensitivity and catalytic activity when compared to Au spheres, nanorods, and hollow spheres (Khalavka et al. 2009). Loading Au nanorods

on the surface of carbon-coated magnetic nanoparticles ($\text{Fe}_3\text{O}_4@\text{C}$ MNPs) further enhances the catalytic activity and exhibits wonderful recyclability and stability. Another factor affecting the catalytic activity is the thickness of the AuNCs wall. Compared the nanocages and nanoboxes, the kinetic data indicate that Au-based nanocages are catalytically more active due to the extremely thin but electrically continuous wall (Zeng et al. 2009). Also, the high content of Au and the accessibility of both outer and inner surfaces through the pores in wall are responsible for high efficient catalysis.

It is reported that branched Au nanostructures can enhance the performance in many reactions (Guerrero-Martínez et al. 2011). In this case, some researchers investigate the catalytic activity of multibranched Au nanoantennas, nanostars, and nanoflowers (Soetan et al. 2016). The results showed that the efficient absorption of 4-NP on the surface of these shapes lied in the shorter protrusions. This is because there are (100) and (110) crystal planes on the shorter protrusions, where had high density of atomic steps and kinks, promoting higher catalytic activity for 4-NP reduction. Hence, it is very important to obtain **Au nanocatalyst** of crystal plane with high index facets.

Please insert **Fig. 14**

In conclusion, the nature of supports has a significant impact on catalytic performance of **Au nanocatalysts**. As for most polymer-supported **Au nanocatalysts**, the shapes of the catalyst can be controlled. Many of them can reduce AuNPs in situ by specific ligands without adding any reducing agent. But the catalytic activity and stability of AuNPs should be further improved. The oxide supported **Au nanocatalysts** like SiO_2 can effectively overcome this because of the confinement effect. With this design, the recycle and stability of **Au nanocatalysts** are greatly enhanced with no Au

leaching. Other metal oxides as supports will form the synergistic effect with Au and the catalytic performance is improved because more active sites are provided. Interestingly, the catalysts are separated easily in the presence of some magnetic metal oxides (Gawande et al. 2014, Shokouhimehr et al. 2018). Nevertheless, the synthetic process is complex and the activity is easier to lose in air. The surface of carbon usually contains a large number of oxygen-containing groups, which benefits the deposition and stability of AuNPs. Some of them possess electron-rich ability and high absorption of organic compounds via π - π stacking interactions, hence increasing the opportunity to access nitroaromatics and AuNPs, improving the catalytic performance, and broadening the application of Au nanocatalysts, especially photocatalysis. Other new supports, such as membrane (Zhong et al. 2018), montmorillonite (Rocha et al. 2018), and molecular sieve (Kusumawati et al. 2018), have been developed and showed highly catalytic performance. The investigation does not just tend to some new supports, but to some new technology like photocatalysis in recent.

7. Comparison with other metal catalysts

Except AuNPs, other metallic NPs including Pd (Shokouhimehr et al. 2013), Pt (Berillo and Cundy 2018), Ag (Wu et al. 2013), Cu (Pi et al. 2018), and Ni (Xia et al. 2018) NPs have also been used for nitroaromatics reduction and the mechanism is similar to that of AuNPs. Just like AuNPs, these free metallic NPs are unstable and easy to aggregate. Accordingly, stabilized metal nanocatalysts are needed and desirable for nitroaromatics reduction (Kim et al. 2015, Shokouhimehr et al. 2014). Among these

well stabilized metallic nanocatalysts, Pd-based nanocatalysts always show the highest catalytic activity for nitroaromatics reduction, even higher than Au nanocatalysts (Deraedt et al. 2014, Shokouhimehr et al. 2018). This is because PdNPs have very strong adsorption for activated hydrogen, which is the rate-limiting step for nitroaromatics reduction (Durand et al. 2008). The catalytic activity is enhanced because of more activated hydrogen. While the rate-limiting step of Au nanocatalyst is the transfer ability of hydrogen to products. Even so, the high catalytic efficiency of Au nanocatalysts under low temperature is still significant. Simultaneously, the low toxicity of Au nanocatalysts is more suitable for practical application.

Ag-based nanocatalysts have widely used in nitroaromatics reduction because of its much lower cost, high activity and selectivity (Ji et al. 2016). However, in most cases, the catalytic activity is not as high as Au nanocatalysts. Besides, the bactericidal ability and toxicity of Ag nanocatalysts cannot be ignored, which will be harmful for beneficial microbes and humans. The other metallic nanocatalysts like Cu and Ni nanocatalysts are very cheap and have also been reported for the reduction of nitroaromatics in these years (Xia et al. 2016, Xiao et al. 2016). But the chemical tolerance and catalytic activity of them are obviously not as good as Au nanocatalysts. In addition, CuNPs also show high propensity for oxidation, which may affect the catalysis.

8. Conclusions, future outlook and challenges

Efficient reduction of nitroaromatics into corresponding amines compounds has paid much attention. Au nanocatalysts can offer an efficient way because of the high catalytic efficiency under low temperature and specific size, synergistic, interfacial, and

shape effects. Due to the trends in size increase of AuNPs when sintering, several synthetic strategies of Au nanocatalyst are widely employed to suppress, including: i) immobilizing or depositing AuNPs on high-surface area substances; ii) encapsulating them in the channels or porous materials; iii) stabilizing them with surface bound ligands. Thus, new green and simple routes of Au nanocatalyst synthetic methods with large loading amount, highly dispersed AuNPs, and wonderful catalytic efficiency for nitroaromatics reduction are still needed. The future outlook and challenges are proposed as follows:

i) Most of studies focus on the synthesis of highly efficient Au nanocatalysts for nitroaromatics reduction but ignore the reason for the high efficient. In addition, the combination of photocatalytic materials is a trend to improve the catalytic performance and energy saving, but the investigation on the mechanism of nitroaromatics reduction under light irradiation should be further developed.

ii) Free AuNPs have high catalytic activity but are easy to aggregate. For this, supported Au nanocatalysts are development, but sometimes the recovery is still limited by unstably interfacial interaction between supports and Au. Thus, the design of core-shell or yolk-shell is a good choice.

iii) For recycle, magnetic materials are usually used as a core to stabilize AuNPs and separate Au nanocatalyst easily, but the magnetic materials only act as a support. Some magnetic metal NPs with the ability to reduce nitroaromatics, such as Ni NPs, can be used to combine with AuNPs to enhance the catalytic performance by bimetallic synergetic effect.

iv) An alternative promising way to enhance the catalytic performance is the synthesis of irregular AuNPs or multi-metallic NPs owing to the edge and corner effects or synergistic effect.

v) Most of works provide efficiently active catalysts, but few of them have been suited to the large-scale industrial use. Thus, synthesis of large-scale industrial used catalysts is needed to further develop.

vi) New materials supported Au nanocatalysts present huge potential in environmental applications. Particularly, a productive way of AuNPs may be combination with other biocompatible materials deposited on different supports either in micro- and nanometer scales. In this manner, metal–organic frameworks system provides a good choice.

vii) Most consideration of researchers is on reducing nitroaromatics in aqueous phase by NaBH₄ solution, further investigation on other medium such as sediment and soil and organic solution is needed to consider.

viii) It is reported that the surface electron density of AuNPs would be somewhat responsible for the catalytic property of some materials like TiO₂ supported Au nanocatalysts (Yang et al. 2016a). The photo-induced electron transfer can further enhance the oxidability of Au nanocatalysts (Yang et al. 2014a). Thus, the electron behavior including electron transfer and density may have effect on the reduction also. In this case, the electron-dependent effect of Au nanocatalysts should be considered in the future work.

ix) For further improvement of the catalytic activity, the single-atom catalyst is deserved to investigate.

955 **Acknowledgement**

956 This study was financially supported by the Program for the National Natural Science
957 Foundation of China (51521006, 51408206, 51579098, 51278176, 51779090,
958 51709101), Science and Technology Plan Project of Hunan Province (2017SK2243),
959 the National Program for Support of Top–Notch Young Professionals of China (2014),
960 the Program for Changjiang Scholars and Innovative Research Team in University
961 (IRT-13R17), the Program for New Century Excellent Talents in University (NCET-13-
962 0186), and Hunan Provincial Science and Technology Plan Project (No.2016RS3026),
963 the Fundamental Research Funds for the Central Universities (531107050978,
964 531107051080).

References

- Aditya, T., Pal, A. and Pal, T. 2015. Nitroarene reduction: a trusted model reaction to test nanoparticle catalysts. *Cheminform* 51, 9410-9431.
- Almukhlifi, H.A. and Burns, R.C. 2015a. Gold nanoparticles on metal oxide surfaces derived from n-alkanethiolate-stabilized gold nanoparticles; investigations of the adsorption mechanism and sulfate formation during subsequent thermolysis. *Appl. Catal., A*. 502, 174-187.
- Almukhlifi, H.A. and Burns, R.C. 2015b. Oxidative dehydrogenation of isobutane to isobutene by pyrovanadates, $M_2V_2O_7$, where $M(II)=Mn, Co, Ni, Cu$ and Zn , and Co_2VO_4 and ZnV_2O_4 : The effect of gold nanoparticles. *J. Mol. Catal. A: Chem.* 408, 26-40.
- Almukhlifi, H.A. and Burns, R.C. 2016a. The complete oxidation of isobutane over CeO_2 and Au/CeO_2 , and the composite catalysts MO_x/CeO_2 and $Au/MO_x/CeO_2$ ($Mn+=Mn, Fe, Co$ and Ni): the effects of gold nanoparticles obtained from n-hexanethiolate-stabilized gold nanoparticles. *J. Mol. Catal. A: Chem.* 415, 131-143.
- Almukhlifi, H.A. and Burns, R.C. 2016b. The effects of gold nanoparticles obtained from the thermolysis of n-hexanethiolate-stabilized gold nanoparticles on isobutane oxidation over metal oxide catalysts. *J. Mol. Catal. A: Chem.* 411, 349-363.
- Ansar, S.M. and Kitchens, C.L. 2016. Impact of gold nanoparticle stabilizing ligands on the colloidal catalytic reduction of 4-nitrophenol. *ACS Catal.* 6, 5553-5560.
- Badwaik, V.D., Bartonjo, J.J., Evans, J.W., Sahi, S.V., Willis, C.B. and Dakshinamurthy, R. 2011. Single-step biofriendly synthesis of surface modifiable, near-spherical gold nanoparticles for applications in biological detection and catalysis. *Langmuir* 27, 5549-5554.
- Barrett, D.H., Scurrell, M.S., Rodella, C.B., Diaz, B., Billing, D.G. and Franklyn, P.J. 2016. Achieving nano-gold stability through rational design. *Chem. Sci.* 7, 6815-6823.
- Berillo, D. and Cundy, A. 2018. 3D-macroporous chitosan-based scaffolds with in situ formed Pd and Pt nanoparticles for nitrophenol reduction. *Carbohydr. Polym.* 192, 166-175.
- Bhosale, M.A., Chenna, D.R. and Bhanage, B.M. 2017. Ultrasound Assisted Synthesis of Gold Nanoparticles as an Efficient Catalyst for Reduction of Various Nitro Compounds. *ChemistrySelect* 2, 1225-1231.
- Biella, S., Prati, L. and Rossi, M. 2002. Selective Oxidation of D-Glucose on Gold Catalyst. *J. Catal.* 206, 242-247.
- Boronat, M., Concepci3n, P., Corma, A., Gonz3lez, S., Illas, F. and Serna, P. 2007. A molecular mechanism for the chemoselective hydrogenation of substituted nitroaromatics with nanoparticles of gold on TiO_2 catalysts: A cooperative effect between gold and the support. *JACS* 129, 16230-16237.
- Boronat, M. and Corma, A. 2010. Origin of the Different Activity and Selectivity toward Hydrogenation of Single Metal Au and Pt on TiO_2 and Bimetallic Au-Pt/ TiO_2 Catalysts. *Langmuir* 26, 16607-16614.
- Cao, Y., Jin, R. and Mirkin, C.A. 2001. DNA-Modified Core-Shell Ag/Au Nanoparticles. *JACS*

1003 123, 7961-7962.

1004 Cao, Z., Chen, H., Zhu, S., Chen, Z., Xu, C., Qi, D. and Ziener, U. 2016. Inverse miniemulsion-
 1005 based preparation of raspberry-like Au/SiO₂ nanocomposite particles with high catalytic
 1006 activity towards reduction of p-nitrophenol. *Colloids Surf., A*. 489, 223-233.

1007 Cárdenas-Lizana, F., De Pedro, Z.M., Gómez-Quero, S., Kiwi-Minsker, L. and Keane, M.A. 2015.
 1008 Carbon supported gold and silver: Application in the gas phase hydrogenation of m-
 1009 dinitrobenzene. *J. Mol. Catal. A: Chem.* 408, 138-146.

1010 Chang, Y.-C. and Chen, D.-H. 2006. Recovery of gold (III) ions by a chitosancoated magnetic nano-
 1011 adsorbent. *Gold Bull.* 39, 98-102.

1012 Chang, Y.-C. and Chen, D.-H. 2009. Catalytic reduction of 4-nitrophenol by magnetically
 1013 recoverable Au nanocatalyst. *J. Hazard. Mater.* 165, 664-669.

1014 Chaplin, B.P., Roundy, E., Guy, K.A., Shapley, J.R. and Werth, C.J. 2006. Effects of natural water
 1015 ions and humic acid on catalytic nitrate reduction kinetics using an alumina supported Pd-Cu
 1016 catalyst. *Environ. Sci. Technol.* 40, 3075-3081.

1017 Chen, J., Xiao, P., Gu, J., Han, D., Zhang, J., Sun, A., Wang, W. and Chen, T. 2014a. A smart hybrid
 1018 system of Au nanoparticle immobilized PDMAEMA brushes for thermally adjustable catalysis.
 1019 *Chem. Commun.* 50, 1212-1214.

1020 Chen, J., Xue, Z., Feng, S., Tu, B. and Zhao, D. 2014b. Synthesis of mesoporous silica hollow
 1021 nanospheres with multiple gold cores and catalytic activity. *J. Colloid Interface Sci.* 429, 62-67.

1022 Chen, M. and Goodman, D.W. 2006. Catalytically active gold: from nanoparticles to ultrathin films.
 1023 *Acc. Chem. Res.* 39, 739-746.

1024 Chen, M., Xu, P., Zeng, G., Yang, C., Huang, D. and Zhang, J. 2015. Bioremediation of soils
 1025 contaminated with polycyclic aromatic hydrocarbons, petroleum, pesticides, chlorophenols and
 1026 heavy metals by composting: applications, microbes and future research needs. *Biotechnol. Adv.*
 1027 33, 745-755.

1028 Chen, S., Wang, T., Yao, Y. and Wei, A. 2018. Facile synthesis of novel fibrous silica@apatite@Au
 1029 composites with superior photo-catalytic activity. *Mater. Des.* 147, 106-113.

1030 Chen, Y., Qiu, J., Wang, X. and Xiu, J. 2006. Preparation and application of highly dispersed gold
 1031 nanoparticles supported on silica for catalytic hydrogenation of aromatic nitro compounds. *J.*
 1032 *Catal.* 242, 227-230.

1033 Cheng, M., Zeng, G., Huang, D., Lai, C., Xu, P., Zhang, C. and Liu, Y. 2016a. Hydroxyl radicals
 1034 based advanced oxidation processes (AOPs) for remediation of soils contaminated with organic
 1035 compounds: a review. *Chem. Eng. J.* 284, 582-598.

1036 Cheng, M., Zeng, G., Huang, D., Lai, C., Xu, P., Zhang, C., Liu, Y., Wan, J., Gong, X. and Zhu, Y.
 1037 2016b. Degradation of atrazine by a novel Fenton-like process and assessment the influence on
 1038 the treated soil. *J. Hazard. Mater.* 312, 184-191.

1039 Cheng, M., Zeng, G., Huang, D., Yang, C., Lai, C., Zhang, C. and Liu, Y. 2017. Advantages and
 1040 challenges of Tween 80 surfactant-enhanced technologies for the remediation of soils
 1041 contaminated with hydrophobic organic compounds. *Chem. Eng. J.* 314, 98-113.

- Cheng, Y., He, H., Yang, C., Zeng, G., Li, X., Chen, H. and Yu, G. 2016c. Challenges and solutions for biofiltration of hydrophobic volatile organic compounds. *Biotechnol. Adv.* 34, 1091-1102.
- Chiu, C.-Y., Chung, P.-J., Lao, K.-U., Liao, C.-W. and Huang, M.H. 2012. Facet-dependent catalytic activity of gold nanocubes, octahedra, and rhombic dodecahedra toward 4-nitroaniline reduction. *J. Phys. Chem. C* 116, 23757-23763.
- Chung, M.W., Cha, I.Y., Ha, M.G., Na, Y., Hwang, J., Ham, H.C., Kim, H.-J., Henkensmeier, D., Yoo, S.J., Kim, J.Y., Lee, S.Y., Park, H.S. and Jang, J.H. 2018. Enhanced CO₂ reduction activity of polyethylene glycol-modified Au nanoparticles prepared via liquid medium sputtering. *Appl. Catal., B* 237, 673-680.
- Conte, M., Miyamura, H., Kobayashi, S. and Chechik, V. 2009. Spin trapping of Au–H intermediate in the alcohol oxidation by supported and unsupported gold catalysts. *JACS* 131, 7189-7196.
- Corma, A., Concepción, P. and Serna, P. 2007. A Different Reaction Pathway for the Reduction of Aromatic Nitro Compounds on Gold Catalysts. *Angew. Chem.* 119, 7404-7407.
- Corma, A. and Serna, P. 2006. Chemoselective hydrogenation of nitro compounds with supported gold catalysts. *Science* 313, 332-334.
- Damato, T.C., de Oliveira, C.C., Ando, R.A. and Camargo, P.H. 2013. A facile approach to TiO₂ colloidal spheres decorated with Au nanoparticles displaying well-defined sizes and uniform dispersion. *Langmuir* 29, 1642-1649.
- Das, S.K., Dickinson, C., Lafir, F., Brougham, D.F. and Marsili, E. 2012. Synthesis, characterization and catalytic activity of gold nanoparticles biosynthesized with *Rhizopus oryzae* protein extract. *Green Chem.* 14, 1322-1334.
- Deng, J.-H., Zhang, X.-R., Zeng, G.-M., Gong, J.-L., Niu, Q.-Y. and Liang, J. 2013. Simultaneous removal of Cd (II) and ionic dyes from aqueous solution using magnetic graphene oxide nanocomposite as an adsorbent. *Chem. Eng. J.* 226, 189-200.
- Deraedt, C., Salmon, L. and Astruc, D. 2014. “Click” Dendrimer-Stabilized Palladium Nanoparticles as a Green Catalyst Down to Parts per Million for Efficient C=C Cross-Coupling Reactions and Reduction of 4-Nitrophenol. *Adv. Synth. Catal.* 356, 2525-2538.
- Downing, R., Kunkeler, P. and Van Bekkum, H. 1997. Catalytic syntheses of aromatic amines. *Catal. Today* 37, 121-136.
- Durand, J., Teuma, E. and Gómez, M. 2008. An Overview of Palladium Nanocatalysts: Surface and Molecular Reactivity. *Eur. J. Inorg. Chem.* 2008, 3577-3586.
- Dykman, L. and Khlebtsov, N. 2012. Gold nanoparticles in biomedical applications: recent advances and perspectives. *Chem. Soc. Rev.* 41, 2256-2282.
- Fang, W., Deng, Y., Tang, L., Zeng, G., Zhou, Y., Xie, X., Wang, J., Wang, Y. and Wang, J. 2017. Synthesis of Pd/Au bimetallic nanoparticle-loaded ultrathin graphitic carbon nitride nanosheets for highly efficient catalytic reduction of p-nitrophenol. *J. Colloid Interface Sci.* 490, 834-843.
- Fenger, R., Fertitta, E., Kirmse, H., Thunemann, A.F. and Rademann, K. 2012. Size dependent catalysis with CTAB-stabilized gold nanoparticles. *Phys. Chem. Chem. Phys.* 14, 9343-9349.
- Fountoulaki, S., Daikopoulou, V., Gkizis, P.L., Tamiolakis, I., Armatas, G.S. and Lykakis, I.N. 2014.

- Mechanistic studies of the reduction of nitroarenes by NaBH₄ or hydrosilanes catalyzed by supported gold nanoparticles. *ACS Catal.* 4, 3504-3511.
- Fu, J., Wang, S., Zhu, J., Wang, K., Gao, M., Wang, X. and Xu, Q. 2018. Au-Ag bimetallic nanoparticles decorated multi-amino cyclophosphazene hybrid microspheres as enhanced activity catalysts for the reduction of 4-nitrophenol. *Mater. Chem. Phys.* 207, 315-324.
- Fu, Y., Huang, T., Jia, B., Zhu, J. and Wang, X. 2017. Reduction of nitrophenols to aminophenols under concerted catalysis by Au/gC₃N₄ contact system. *Appl. Catal., B.* 202, 430-437.
- Gangula, A., Podila, R., M, R., Karanam, L., Janardhana, C. and Rao, A.M. 2011. Catalytic Reduction of 4-Nitrophenol using Biogenic Gold and Silver Nanoparticles Derived from *Breynia rhamnoides*. *Langmuir* 27, 15268-15274.
- Gawande, M.B., Rath, A.K., Tucek, J., Safarova, K., Bundaleski, N., Teodoro, O.M.N.D., Kvitek, L., Varma, R.S. and Zboril, R. 2014. Magnetic gold nanocatalyst (nanocat-Fe-Au): catalytic applications for the oxidative esterification and hydrogen transfer reactions. *Green Chem.* 16, 4137-4143.
- Ge, J., Huynh, T., Hu, Y. and Yin, Y. 2008. Hierarchical magnetite/silica nanoassemblies as magnetically recoverable catalyst-supports. *Nano Lett.* 8, 931-934.
- Geim, A.K. 2009. Graphene: status and prospects. *science* 324, 1530-1534.
- Godfrey, I.J., Dent, A.J., Parkin, I.P., Maenosono, S. and Sankar, G. 2017. Structure of Gold-Silver Nanoparticles. *J. Phys. Chem. C.* 121, 1957-1963.
- Gong, C., Zhou, Z., Li, J., Zhou, H. and Liu, R. 2018. Facile synthesis of ultra stable Fe₃O₄@Carbon core-shell nanoparticles entrapped satellite Au catalysts with enhanced 4-nitrophenol reduction property. *J. Taiwan Inst. Chem. Eng.* 84, 229-235.
- Gong, J.-L., Wang, B., Zeng, G.-M., Yang, C.-P., Niu, C.-G., Niu, Q.-Y., Zhou, W.-J. and Liang, Y. 2009. Removal of cationic dyes from aqueous solution using magnetic multi-wall carbon nanotube nanocomposite as adsorbent. *J. Hazard. Mater.* 164, 1517-1522.
- Gong, J. 2012. Structure and Surface Chemistry of Gold-Based Model Catalysts. *Chem. Rev.* 112, 2987-3054.
- Grisel, R., Slyconish, J. and Nieuwenhuys, B. 2001. Oxidation reactions over multi-component catalysts: low-temperature CO oxidation and the total oxidation of CH₄. *Top. Catal.* 16, 425-431.
- Gu, S., Wunder, S., Lu, Y., Ballauff, M., Fenger, R., Rademann, K., Jaquet, B. and Zacccone, A. 2014. Kinetic Analysis of the Catalytic Reduction of 4-Nitrophenol by Metallic Nanoparticles. *J. Phys. Chem. C.* 118, 18618-18625.
- Guadie Assefa, A., Adugna Mesfin, A., Legesse Akele, M., Kokeb Alemu, A., Gangapuram, B.R., Guttena, V. and Alle, M. 2017. Microwave-Assisted Green Synthesis of Gold Nanoparticles Using Olibanum Gum (*Boswellia serrate*) and its Catalytic Reduction of 4-Nitrophenol and Hexacyanoferrate (III) by Sodium Borohydride. *J. Cluster Sci.* 28, 917-935.
- Guerrero-Martínez, A., Barbosa, S., Pastoriza-Santos, I. and Liz-Marzán, L.M. 2011. Nanostars shine bright for you. *Curr. Opin. Colloid Interface Sci.* 16, 118-127.

- Guo, J. and Suslick, K.S. 2012. Gold nanoparticles encapsulated in porous carbon. *Chem. Commun.* 48, 11094-11096.
- Guo, P., Tang, L., Tang, J., Zeng, G., Huang, B., Dong, H., Zhang, Y., Zhou, Y., Deng, Y. and Ma, L. 2016. Catalytic reduction–adsorption for removal of p-nitrophenol and its conversion p-aminophenol from water by gold nanoparticles supported on oxidized mesoporous carbon. *J. Colloid Interface Sci.* 469, 78-85.
- Gupta, V.K., Atar, N., Yola, M.L., Üstündağ, Z. and Uzun, L. 2014. A novel magnetic Fe@Au core–shell nanoparticles anchored graphene oxide recyclable nanocatalyst for the reduction of nitrophenol compounds. *Water Res.* 48, 210-217.
- Guria, M.K., Majumdar, M. and Bhattacharyya, M. 2016. Green synthesis of protein capped nano-gold particle: An excellent recyclable nano-catalyst for the reduction of nitro-aromatic pollutants at higher concentration. *J. Mol. Liq.* 222, 549-557.
- Hamidouche, S., Bouras, O., Zermane, F., Cheknane, B., Houari, M., Debord, J., Harel, M., Bollinger, J.-C. and Baudu, M. 2015. Simultaneous sorption of 4-nitrophenol and 2-nitrophenol on a hybrid geocomposite based on surfactant-modified pillared-clay and activated carbon. *Chem. Eng. J.* 279, 964-972.
- Han, C.W., Choksi, T., Milligan, C., Majumdar, P., Manto, M., Cui, Y., Sang, X., Unocic, R.R., Zemlyanov, D. and Wang, C. 2017. A Discovery of Strong Metal–Support Bonding in Nanoengineered Au–Fe₃O₄ Dumbbell-like Nanoparticles by in Situ Transmission Electron Microscopy. *Nano Lett.* 17, 4576-4582.
- Haruta, M., Yamada, N., Kobayashi, T. and Iijima, S. 1989. Gold catalysts prepared by coprecipitation for low-temperature oxidation of hydrogen and of carbon monoxide. *J. Catal.* 115, 301-309.
- He, Y., Zhang, N., Zhang, L., Gong, Q., Yi, M., Wang, W., Qiu, H. and Gao, J. 2014. Fabrication of Au–Pd nanoparticles/graphene oxide and their excellent catalytic performance. *Mater. Res. Bull.* 51, 397-401.
- He, Z., Fu, J., Cheng, B., Yu, J. and Cao, S. 2017. Cu₂(OH)₂CO₃ clusters: Novel noble-metal-free cocatalysts for efficient photocatalytic hydrogen production from water splitting. *Appl. Catal., B.* 205, 104-111.
- Hirakawa, H., Shiota, S., Shiraishi, Y., Sakamoto, H., Ichikawa, S. and Hirai, T. 2016. Au Nanoparticles Supported on BiVO₄: Effective Inorganic Photocatalysts for H₂O₂ Production from Water and O₂ under Visible Light. *ACS Catal.* 6, 4976-4982.
- Hu, D., Jin, S., Shi, Y., Wang, X., Graff, R.W., Liu, W., Zhu, M. and Gao, H. 2017. Preparation of hyperstar polymers with encapsulated Au₂₅(SR)₁₈ clusters as recyclable catalysts for nitrophenol reduction. *Nanoscale* 9, 3629-3636.
- Huang, D., Hu, C., Zeng, G., Cheng, M., Xu, P., Gong, X., Wang, R. and Xue, W. 2017a. Combination of Fenton processes and biotreatment for wastewater treatment and soil remediation. *Sci. Total Environ.* 574, 1599-1610.
- Huang, D., Liu, L., Zeng, G., Xu, P., Huang, C., Deng, L., Wang, R. and Wan, J. 2017b. The effects

of rice straw biochar on indigenous microbial community and enzymes activity in heavy metal-contaminated sediment. *Chemosphere* 174, 545-553.

Huang, D., Xue, W., Zeng, G., Wan, J., Chen, G., Huang, C., Zhang, C., Cheng, M. and Xu, P. 2016. Immobilization of Cd in river sediments by sodium alginate modified nanoscale zero-valent iron: Impact on enzyme activities and microbial community diversity. *Water Res.* 106, 15-25.

Huang, X., Guo, C., Zuo, J., Zheng, N. and Stucky, G.D. 2009. An Assembly Route to Inorganic Catalytic Nanoreactors Containing Sub-10-nm Gold Nanoparticles with Anti-Aggregation Properties. *Small* 5, 361-365.

Hutchings, G.J. 1985. Vapor phase hydrochlorination of acetylene: Correlation of catalytic activity of supported metal chloride catalysts. *J. Catal.* 96, 292-295.

Hutchings, G.J. and Haruta, M. 2005. A golden age of catalysis: A perspective. *Appl. Catal., A* 291, 2-5.

Jan, J.-S., Chuang, T.-H., Chen, P.-J. and Teng, H. 2011. Layer-by-layer polypeptide macromolecular assemblies-mediated synthesis of mesoporous silica and gold nanoparticle/mesoporous silica tubular nanostructures. *Langmuir* 27, 2834-2843.

Jayabal, S. and Ramaraj, R. 2014. Bimetallic Au/Ag nanorods embedded in functionalized silicate sol-gel matrix as an efficient catalyst for nitrobenzene reduction. *Appl. Catal., A* 470, 369-375.

Ji, T., Chen, L., Mu, L., Yuan, R., Knoblauch, M., Bao, F.S. and Zhu, J. 2016. In-situ reduction of Ag nanoparticles on oxygenated mesoporous carbon fabric: Exceptional catalyst for nitroaromatics reduction. *Appl. Catal., B* 182, 306-315.

Jiang, L., Yuan, X., Zeng, G., Chen, X., Wu, Z., Liang, J., Zhang, J., Wang, H. and Wang, H. 2017. Phosphorus- and Sulfur-Codoped g-C₃N₄: Facile Preparation, Mechanism Insight, and Application as Efficient Photocatalyst for Tetracycline and Methyl Orange Degradation under Visible Light Irradiation. *ACS Sustain. Chem. Eng.* 5, 5831-5841.

Ju, Y., Li, X., Feng, J., Ma, Y., Hu, J. and Chen, X. 2014. One pot in situ growth of gold nanoparticles on amine-modified graphene oxide and their high catalytic properties. *Appl. Surf. Sci.* 316, 132-140.

Kadam, H.K. and Tilve, S.G. 2015. Advancement in methodologies for reduction of nitroarenes. *Rsc Adv.* 5, 83391-83407.

Khalavka, Y., Becker, J. and Sonnichsen, C. 2009. Synthesis of rod-shaped gold nanorattles with improved plasmon sensitivity and catalytic activity. *JACS* 131, 1871-1875.

Khoudiakov, M., Gupta, M.C. and Deevi, S. 2005. Au/Fe₂O₃ nanocatalysts for CO oxidation: a comparative study of deposition-precipitation and coprecipitation techniques. *Appl. Catal., A* 291, 151-161.

Kim, A., Rafiaei, S.M., Abolhosseini, S. and Shokouhimehr, M. 2015. Palladium Nanocatalysts Confined in Mesoporous Silica for Heterogeneous Reduction of Nitroaromatics. *Energy Environ. Focus* 4, 18-23(16).

Koklioti, M.A., Skaltsas, T., Sato, Y., Suenaga, K., Stergiou, A. and Tagmatarchis, N. 2017. Mechanistic insights into the photocatalytic properties of metal nanocluster/graphene ensembles.

1198 Examining the role of visible light in the reduction of 4-nitrophenol. *Nanoscale* 9, 9685-9692.

1199 Kong, W., Huang, D., Xu, G., Ren, J., Liu, C., Zhao, L. and Sun, R. 2016. Graphene
 1200 Oxide/Polyacrylamide/Aluminum Ion Cross-Linked Carboxymethyl Hemicellulose
 1201 Nanocomposite Hydrogels with Very Tough and Elastic Properties. *Chem-Asian J.* 11, 1697-
 1202 1704.

1203 Kuroda, K., Ishida, T. and Haruta, M. 2009. Reduction of 4-nitrophenol to 4-aminophenol over Au
 1204 nanoparticles deposited on PMMA. *J. Mol. Catal. A: Chem.* 298, 7-11.

1205 Kusumawati, E.N., Nishio-Hamane, D. and Sasaki, T. 2018. Size-controllable gold nanoparticles
 1206 prepared from immobilized gold-containing ionic liquids on SBA-15. *Catal. Today* 309, 109-
 1207 118.

1208 Lai, C., Lei, Q., Guangming, Z., Yunguo, L., Danlian, H., Chen, Z., Piao, X., Min, C., Xiangbin, Q.
 1209 and Manman, W. 2015. Sensitive and selective detection of mercury ions based on papain and
 1210 2,6-pyridinedicarboxylic acid functionalized gold nanoparticles. *Rsc Adv.* 6, 3259-3266.

1211 Lai, C., Liu, X., Qin, L., Zhang, C., Zeng, G., Huang, D., Cheng, M., Xu, P., Yi, H. and Huang, D.
 1212 2017. Chitosan-wrapped gold nanoparticles for hydrogen-bonding recognition and colorimetric
 1213 determination of the antibiotic kanamycin. *Microchim. Acta*, 1-9.

1214 Lai, C., Wang, M.-M., Zeng, G.-M., Liu, Y.-G., Huang, D.-L., Zhang, C., Wang, R.-Z., Xu, P., Cheng,
 1215 M. and Huang, C. 2016. Synthesis of surface molecular imprinted TiO₂/graphene photocatalyst
 1216 and its highly efficient photocatalytic degradation of target pollutant under visible light
 1217 irradiation. *Appl. Surf. Sci.* 390, 368-376.

1218 Layek, K., Kantam, M.L., Shirai, M., Nishio-Hamane, D., Sasaki, T. and Maheswaran, H. 2012.
 1219 Gold nanoparticles stabilized on nanocrystalline magnesium oxide as an active catalyst for
 1220 reduction of nitroarenes in aqueous medium at room temperature. *Green Chem.* 14, 3164-3174.

1221 Le, X., Dong, Z., Zhang, W., Li, X. and Ma, J. 2014. Fibrous nano-silica containing immobilized
 1222 Ni@Au core-shell nanoparticles: A highly active and reusable catalyst for the reduction of 4-
 1223 nitrophenol and 2-nitroaniline. *J. Mol. Catal. A: Chem.* 395, 58-65.

1224 Lee, J., Park, J.C. and Song, H. 2008. A Nanoreactor Framework of a Au@SiO₂ Yolk/Shell
 1225 Structure for Catalytic Reduction of p-Nitrophenol. *Adv. Mater.* 20, 1523-1528.

1226 Lee, Y., Garcia, M.A., Frey Huls, N.A. and Sun, S. 2010. Synthetic tuning of the catalytic properties
 1227 of Au - Fe₃O₄ nanoparticles. *Angew. Chem.* 122, 1293-1296.

1228 Li, B., Hao, Y., Shao, X., Tang, H., Wang, T., Zhu, J. and Yan, S. 2015. Synthesis of hierarchically
 1229 porous metal oxides and Au/TiO₂ nanohybrids for photodegradation of organic dye and catalytic
 1230 reduction of 4-nitrophenol. *J. Catal.* 329, 368-378.

1231 Li, B., Lai, C., Zeng, G., Qin, L., Yi, H., Huang, D., Zhou, C., Liu, X., Cheng, M., Xu, P., Zhang,
 1232 C., Huang, F. and Liu, S. 2018a. Facile Hydrothermal Synthesis of Z-Scheme Bi₂Fe₄O₉/Bi₂WO₆
 1233 Heterojunction Photocatalyst with Enhanced Visible Light Photocatalytic Activity. *ACS Appl.*
 1234 *Mater. Interfaces* 10, 18824-18836.

1235 Li, J., Liu, C.-y. and Liu, Y. 2012. Au/graphene hydrogel: synthesis, characterization and its use for
 1236 catalytic reduction of 4-nitrophenol. *J. Mater. Chem.* 22, 8426-8430.

- Li, J., Song, S., Long, Y., Yao, S., Ge, X., Wu, L., Zhang, Y., Wang, X., Yang, X. and Zhang, H. 2018b. A General One-pot Strategy for the Synthesis of Au@multi-oxides Yolk@shell Nanospheres with Enhanced Catalytic Performance. *Chem. Sci.*
- Li, M. and Chen, G. 2013. Revisiting catalytic model reaction p-nitrophenol/ NaBH_4 using metallic nanoparticles coated on polymeric spheres. *Nanoscale* 5, 11919-11927.
- Li, N., Zhao, P. and Astruc, D. 2014. Anisotropic Gold Nanoparticles: Synthesis, Properties, Applications, and Toxicity. *Angew. Chem. Int. Ed.* 53, 1756-1789.
- Li, X., Ma, Y., Yang, Z., Huang, D., Xu, S., Wang, T., Su, Y., Hu, N. and Zhang, Y. 2017. In situ preparation of magnetic Ni-Au/graphene nanocomposites with electron-enhanced catalytic performance. *J. Alloys Compd.* 706, 377-386.
- Liang, J., Yang, Z., Tang, L., Zeng, G., Yu, M., Li, X., Wu, H., Qian, Y., Li, X. and Luo, Y. 2017. Changes in heavy metal mobility and availability from contaminated wetland soil remediated with combined biochar-compost. *Chemosphere* 181, 281-288.
- Lim, X. 2016. The new breed of cutting-edge catalysts. *Nature News* 537, 156.
- Lin, F.-h. and Doong, R.-a. 2011. Bifunctional Au- Fe_3O_4 Heterostructures for Magnetically Recyclable Catalysis of Nitrophenol Reduction. *J. Phys. Chem. C.* 115, 6591-6598.
- Lin, F.-h. and Doong, R.-a. 2017. Catalytic Nanoreactors of Au@ Fe_3O_4 Yolk-Shell Nanostructures with Various Au Sizes for Efficient Nitroarene Reduction. *J. Phys. Chem. C.* 121, 7844-7853.
- Lin, S. and Vannice, M.A. 1991. Gold dispersed on TiO_2 and SiO_2 : adsorption properties and catalytic behavior in hydrogenation reactions. *Catal. Lett.* 10, 47-61.
- Lin, S.D., Bollinger, M. and Vannice, M.A. 1993. Low temperature CO oxidation over Au/ TiO_2 and Au/ SiO_2 catalysts. *Catal. Lett.* 17, 245-262.
- Lin, Y., Qiao, Y., Wang, Y., Yan, Y. and Huang, J. 2012. Self-assembled laminated nanoribbon-directed synthesis of noble metallic nanoparticle-decorated silica nanotubes and their catalytic applications. *J. Mater. Chem.* 22, 18314-18320.
- Liu, B., Yang, M. and Li, H. 2017a. Synthesis of gold nanoflowers assisted by a CH-CF hybrid surfactant and their applications in SERS and catalytic reduction of 4-nitroaniline. *Colloids Surf., A.* 520, 213-221.
- Liu, H., Wang, J., Feng, Z., Lin, Y., Zhang, L. and Su, D. 2015. Facile Synthesis of Au Nanoparticles Embedded in an Ultrathin Hollow Graphene Nanoshell with Robust Catalytic Performance. *Small* 11, 5059-5064.
- Liu, X., Su, Y., Lang, J., Chai, Z. and Wang, X. 2017b. A novel Au-loaded $\text{Na}_2\text{Ta}_2\text{O}_6$ multifunctional catalyst: Thermocatalytic and photocatalytic elimination of the poisonous nitrobenzene derivatives from wastewater under natural condition. *J. Alloys Compd.* 695, 60-69.
- Liu, Y., Li, M. and Chen, G. 2013. A new type of raspberry-like polymer composite sub-microspheres with tunable gold nanoparticles coverage and their enhanced catalytic properties. *Journal of Materials Chemistry A* 1, 930-937.
- Long, F., Gong, J.-L., Zeng, G.-M., Chen, L., Wang, X.-Y., Deng, J.-H., Niu, Q.-Y., Zhang, H.-Y. and Zhang, X.-R. 2011. Removal of phosphate from aqueous solution by magnetic Fe-Zr binary

oxide. Chem. Eng. J. 171, 448-455.

1277 Lv, J.-J., Wang, A.-J., Ma, X., Xiang, R.-Y., Chen, J.-R. and Feng, J.-J. 2015. One-pot synthesis of
 1278 porous Pt-Au nanodendrites supported on reduced graphene oxide nanosheets toward catalytic
 1279 reduction of 4-nitrophenol. J. Mater. Chem. A. 3, 290-296.

1280 Ma, C., Xue, W., Li, J., Xing, W. and Hao, Z. 2013. Mesoporous carbon-confined Au catalysts with
 1281 superior activity for selective oxidation of glucose to gluconic acid. Green Chem. 15, 1035-1041.

1282 Ma, T., Yang, W., Liu, S., Zhang, H. and Liang, F. 2017. A Comparison Reduction of 4-Nitrophenol
 1283 by Gold Nanospheres and Gold Nanostars. Catalysts 7, 38.

1284 Maicu, M., Hidalgo, M.C., Colón, G. and Navío, J.A. 2011. Comparative study of the
 1285 photodeposition of Pt, Au and Pd on pre-sulphated TiO₂ for the photocatalytic decomposition
 1286 of phenol. J. Photochem. Photobiol., A. 217, 275-283.

1287 Maji, S.K. and Jana, A. 2017. Two-dimensional nanohybrid (RGS@AuNPs) as an effective catalyst
 1288 for the reduction of 4-nitrophenol and photo-degradation of methylene blue dye. New J. Chem.
 1289 41, 3326-3332.

1290 Matsushima, Y., Nishiyabu, R., Takanashi, N., Haruta, M., Kimura, H. and Kubo, Y. 2012. Boronate
 1291 self-assemblies with embedded Au nanoparticles: preparation, characterization and their
 1292 catalytic activities for the reduction of nitroaromatic compounds. J. Mater. Chem. 22, 24124-
 1293 24131.

1294 Manuel, S., Léger, B., Addad, A., Monflier, E. and Hapiot, F. 2016. Cyclodextrins as effective
 1295 additives in AuNP-catalyzed reduction of nitrobenzene derivatives in a ball-mill. Green Chem.
 1296 18, 5500-5509.

1297 Miah, A.T., Bharadwaj, S.K. and Saikia, P. 2017. Surfactant free synthesis of gold nanoparticles
 1298 within meso-channels of non-functionalized SBA-15 for its promising catalytic activity. Powder
 1299 Technol. 315, 147-156.

1300 Mitsudome, T. and Kaneda, K. 2013. Gold nanoparticle catalysts for selective hydrogenations.
 1301 Green Chem. 15, 2636-2654.

1302 Mitsudome, T., Yamamoto, M., Maeno, Z., Mizugaki, T., Jitsukawa, K. and Kaneda, K. 2015. One-
 1303 step synthesis of core-gold/shell-ceria nanomaterial and its catalysis for highly selective
 1304 semihydrogenation of alkynes. JACS 137, 13452-13455.

1305 Moghaddam, F.M., Ayati, S.E., Firouzi, H.R., Hosseini, S.H. and Pourjavadi, A. 2017. Gold
 1306 nanoparticles anchored onto the magnetic poly(ionic-liquid) polymer as robust and recoverable
 1307 catalyst for reduction of Nitroarenes. Appl. Organomet. Chem. 31, n/a-n/a.

1308 Narayanan, K.B. and Sakthivel, N. 2011. Synthesis and characterization of nano-gold composite
 1309 using *Cylindrocladium floridanum* and its heterogeneous catalysis in the degradation of 4-
 1310 nitrophenol. J. Hazard. Mater. 189, 519-525.

1311 Nehl, C.L. and Hafner, J.H. 2008. Shape-dependent plasmon resonances of gold nanoparticles. J.
 1312 Mater. Chem. 18, 2415-2419.

1313 Nguyen, V., Cai, Q. and Grimes, C.A. 2016. Towards efficient visible-light active photocatalysts:
 1314 CdS/Au sensitized TiO₂ nanotube arrays. J. Colloid Interface Sci. 483, 287-294.

- Nigra, M.M., Ha, J.-M. and Katz, A. 2013. Identification of site requirements for reduction of 4-nitrophenol using gold nanoparticle catalysts. *Catal. Sci. Technol.* 3, 2976-2983.
- Noschese, A., Buonerba, A., Canton, P., Milione, S., Capacchione, C. and Grassi, A. 2016. Highly efficient and selective reduction of nitroarenes into anilines catalyzed by gold nanoparticles incarcerated in a nanoporous polymer matrix: Role of the polymeric support and insight into the reaction mechanism. *J. Catal.* 340, 30-40.
- Novoselov, K.S., Geim, A.K., Morozov, S.V., Jiang, D., Zhang, Y., Dubonos, S.V., Grigorieva, I.V. and Firsov, A.A. 2004. Electric Field Effect in Atomically Thin Carbon Films. *Science* 306, 666.
- Nutt, M.O., Heck, K.N., Alvarez, P. and Wong, M.S. 2006. Improved Pd-on-Au bimetallic nanoparticle catalysts for aqueous-phase trichloroethene hydrodechlorination. *Appl. Catal., B.* 69, 115-125.
- Pan, M., Brush, A.J., Pozun, Z.D., Ham, H.C., Yu, W.-Y., Henkelman, G., Hwang, G.S. and Mullins, C.B. 2013. Model studies of heterogeneous catalytic hydrogenation reactions with gold. *Chem. Soc. Rev.* 42, 5002-5013.
- Panigrahi, S., Basu, S., Praharaj, S., Pande, S., Jana, S., Pal, A., Ghosh, S.K. and Pal, T. 2007. Synthesis and size-selective catalysis by supported gold nanoparticles: study on heterogeneous and homogeneous catalytic process. *J. Phys. Chem. C.* 111, 4596-4605.
- Pi, D., Zhou, H., Zhou, Y., Liu, Q., He, R., Shen, G. and Uozumi, Y. 2018. Cu-catalyzed reduction of azaarenes and nitroaromatics with diboronic acid as reductant. *Tetrahedron* 74, 2121-2129.
- Pocklanova, R., Rathi, A.K., Gawande, M.B., Datta, K.K.R., Ranc, V., Cepe, K., Petr, M., Varma, R.S., Kvitek, L. and Zboril, R. 2016. Gold nanoparticle-decorated graphene oxide: Synthesis and application in oxidation reactions under benign conditions. *J. Mol. Catal. A: Chem.* 424, 121-127.
- Pozun, Z.D., Rodenbusch, S.E., Keller, E., Tran, K., Tang, W., Stevenson, K.J. and Henkelman, G. 2013. A systematic investigation of p-nitrophenol reduction by bimetallic dendrimer encapsulated nanoparticles. *J. Phys. Chem. C.* 117, 7598-7604.
- Prati, L. and Martra, G. 1999. New gold catalysts for liquid phase oxidation. *Gold Bull.* 32, 96-101.
- Premkumar, T., Lee, K. and Geckeler, K.E. 2011. Shape-tailoring and catalytic function of anisotropic gold nanostructures. *Nanoscale Res. Lett.* 6, 547.
- Pretzer, L.A., Heck, K.N., Kim, S.S., Fang, Y.-L., Zhao, Z., Guo, N., Wu, T., Miller, J.T. and Wong, M.S. 2016. Improving gold catalysis of nitroarene reduction with surface Pd. *Catal. Today* 264, 31-36.
- Pyykko, P. 1988. Relativistic effects in structural chemistry. *Chem. Rev.* 88, 563-594.
- Qi, P., Chen, S., Chen, J., Zheng, J., Zheng, X. and Yuan, Y. 2015. Catalysis and reactivation of ordered mesoporous carbon-supported gold nanoparticles for the base-free oxidation of glucose to gluconic acid. *ACS Catal.* 5, 2659-2670.
- Qian, H., Zhao, Z., Velazquez, J.C., Pretzer, L.A., Heck, K.N. and Wong, M.S. 2014. Supporting palladium metal on gold nanoparticles improves its catalysis for nitrite reduction. *Nanoscale* 6, 358-364.

- Qin, L., Huang, D., Xu, P., Zeng, G., Lai, C., Fu, Y., Yi, H., Li, B., Zhang, C., Cheng, M., Zhou, C. and Wen, X. 2019. In-situ deposition of gold nanoparticles onto polydopamine-decorated g-C₃N₄ for highly efficient reduction of nitroaromatics in environmental water purification. *J. Colloid Interface Sci.* 534, 357-369.
- Qin, L., Zeng, G., Lai, C., Huang, D., Xu, P., Zhang, C., Cheng, M., Liu, X., Liu, S. and Li, B. 2018. "Gold rush" in modern science: Fabrication strategies and typical advanced applications of gold nanoparticles in sensing. *Coord. Chem. Rev.* 359, 1-31.
- Qin, L., Zeng, G., Lai, C., Huang, D., Zhang, C., Xu, P., Hu, T., Liu, X., Cheng, M. and Liu, Y. 2017. A visual application of gold nanoparticles: Simple, reliable and sensitive detection of kanamycin based on hydrogen-bonding recognition. *Sens. Actuators, B* 243, 946-954.
- Qiu, L., Peng, Y., Liu, B., Lin, B., Peng, Y., Malik, M.J. and Yan, F. 2012. Polypyrrole nanotube-supported gold nanoparticles: An efficient electrocatalyst for oxygen reduction and catalytic reduction of 4-nitrophenol. *Appl. Catal., A* 413, 230-237.
- Qiu, P., Xu, C., Zhou, N., Chen, H. and Jiang, F. 2018. Metal-free black phosphorus nanosheets-decorated graphitic carbon nitride nanosheets with CP bonds for excellent photocatalytic nitrogen fixation. *Appl. Catal., B* 221, 27-35.
- Qu, Y., Pei, X., Shen, W., Zhang, X., Wang, J., Zhang, Z., Li, S., You, S., Ma, F. and Zhou, J. 2017. Biosynthesis of gold nanoparticles by *Aspergillum* sp. WL-Au for degradation of aromatic pollutants. *Physica E* 88, 133-141.
- Que, Y., Feng, C., Zhang, S. and Huang, X. 2015. Stability and catalytic activity of PEG-b-PS-capped gold nanoparticles: a matter of PS chain length. *J. Phys. Chem. C* 119, 1960-1970.
- Rafatullah, M., Sulaiman, O., Hashim, R. and Ahmad, A. 2010. Adsorption of methylene blue on low-cost adsorbents: a review. *J. Hazard. Mater.* 177, 70-80.
- Ramirez, O., Bonard, S.n., Saldías, C., Radic, D. and Leiva, A.n. 2017. Biobased Chitosan Nanocomposite Films Containing Gold Nanoparticles: Obtainment, Characterization, and Catalytic Activity Assessment. *ACS Appl. Mater. Interfaces* 9, 16561-16570.
- Rashid, M.H. and Mandal, T.K. 2008. Templateless Synthesis of Polygonal Gold Nanoparticles: An Unsupported and Reusable Catalyst with Superior Activity. *Adv. Funct. Mater.* 18, 2261-2271.
- Rocha, M., Costa, P., Sousa, C.A.D., Pereira, C., Rodríguez-Borges, J.E. and Freire, C. 2018. L-serine-functionalized montmorillonite decorated with Au nanoparticles: A new highly efficient catalyst for the reduction of 4-nitrophenol. *J. Catal.* 361, 143-155.
- Rodríguez-Reinoso, F. 1998. The role of carbon materials in heterogeneous catalysis. *Carbon* 36, 159-175.
- Rout, L., Kumar, A., Dhaka, R.S., Reddy, G.N., Giri, S. and Dash, P. 2017. Bimetallic Au-Cu alloy nanoparticles on reduced graphene oxide support: Synthesis, catalytic activity and investigation of synergistic effect by DFT analysis. *Appl. Catal., A* 538, 107-122.
- Saha, S., Pal, A., Kundu, S., Basu, S. and Pal, T. 2009. Photochemical green synthesis of calcium-alginate-stabilized Ag and Au nanoparticles and their catalytic application to 4-nitrophenol reduction. *Langmuir* 26, 2885-2893.

- Sahoo, A., Tripathy, S.K., Dehury, N. and Patra, S. 2015. A porous trimetallic Au@Pd@Ru nanoparticle system: synthesis, characterisation and efficient dye degradation and removal. *J. Mater. Chem. A*. 3, 19376-19383.
- Sau, T.K., Pal, A. and Pal, T. 2001. Size regime dependent catalysis by gold nanoparticles for the reduction of eosin. *J. Phys. Chem. B*. 105, 9266-9272.
- Scurrrell, M.S. 2017. Thoughts on the use of gold-based catalysts in environmental protection catalysis. *Gold Bull.* 50, 77-84.
- Sharma, N.C., Sahi, S.V., Nath, S., Parsons, J.G., Gardea- Torresde, J.L. and Pal, T. 2007. Synthesis of Plant-Mediated Gold Nanoparticles and Catalytic Role of Biomatrix-Embedded Nanomaterials. *Environ. Sci. Technol.* 41, 5137-5142.
- Shen, J., Zhou, Y., Huang, J., Zhu, Y., Zhu, J., Yang, X., Chen, W., Yao, Y., Qian, S., Jiang, H. and Li, C. 2017a. In-situ SERS monitoring of reaction catalyzed by multifunctional Fe₃O₄@TiO₂@Ag-Au microspheres. *Appl. Catal., B*. 205, 11-18.
- Shen, W., Qu, Y., Pei, X., Li, S., You, S., Wang, J., Zhang, Z. and Zhou, J. 2017b. Catalytic reduction of 4-nitrophenol using gold nanoparticles biosynthesized by cell-free extracts of *Aspergillus* sp. WL-Au. *J. Hazard. Mater.* 321, 299-306.
- Shen, W., Qu, Y., Pei, X., Zhang, X., Ma, Q., Zhang, Z., Li, S. and Zhou, J. 2016. Green synthesis of gold nanoparticles by a newly isolated strain *Trichosporon montevidense* for catalytic hydrogenation of nitroaromatics. *Biotechnol. Lett* 38, 1503-1508.
- Shi, C., Zhu, N., Cao, Y. and Wu, P. 2015. Biosynthesis of gold nanoparticles assisted by the intracellular protein extract of *Pycnoporus sanguineus* and its catalysis in degradation of 4-nitroaniline. *Nanoscale Res. Lett.* 10, 1-8.
- Shi, H., Xu, N., Zhao, D. and Xu, B.-Q. 2008. Immobilized PVA-stabilized gold nanoparticles on silica show an unusual selectivity in the hydrogenation of cinnamaldehyde. *Catal. Commun.* 9, 1949-1954.
- Shimizu, K.-i., Miyamoto, Y., Kawasaki, T., Tanji, T., Tai, Y. and Satsuma, A. 2009. Chemoselective hydrogenation of nitroaromatics by supported gold catalysts: mechanistic reasons of size-and support-dependent activity and selectivity. *J. Phys. Chem. C*. 113, 17803-17810.
- Shokouhimehr, M., Hong, K., Lee, T.H., Moon, C.W., Hong, S.P., Zhang, K., Suh, J.M., Choi, K.S., Varma, R.S. and Jang, H.W. 2018. Magnetically retrievable nanocomposite adorned with Pd nanocatalysts: efficient reduction of nitroaromatics in aqueous media. *Green Chem.* 20, 3809-3817.
- Shokouhimehr, M., Kim, T., Jun, S.W., Shin, K., Jang, Y., Kim, B.H., Kim, J. and Hyeon, T. 2014. Magnetically separable carbon nanocomposite catalysts for efficient nitroarene reduction and Suzuki reactions. *Appl. Catal., A*. 476, 133-139.
- Shokouhimehr, M., Lee, J.E., Han, S.I. and Hyeon, T. 2013. Magnetically recyclable hollow nanocomposite catalysts for heterogeneous reduction of nitroarenes and Suzuki reactions. *Chem. Commun.* 49, 4779-4781.
- Si, R., Liu, J., Zhang, Y., Chen, X., Dai, W. and Fu, X. 2016. Comparative study on the effect of H₂

pre-adsorption on CO oxidation in O₂-poor atmosphere over Au/TiO₂ and TiO₂: Temperature programmed surface reaction by a multiplexed mass spectrometer testing. *Appl. Surf. Sci.* 387, 1062-1071.

Sinatra, L., LaGrow, A.P., Peng, W., Kirmani, A.R., Amassian, A., Idriss, H. and Bakr, O.M. 2015. A Au/Cu₂O–TiO₂ system for photo-catalytic hydrogen production. A pn-junction effect or a simple case of in situ reduction? *J. Catal.* 322, 109-117.

Soetan, N., Zarick, H.F., Banks, C., Webb, J.A., Libson, G., Coppola, A. and Bardhan, R. 2016. Morphology-directed catalysis with branched gold nanoantennas. *J. Phys. Chem. C.* 120, 10320-10327.

Solsona, B., Garc ía, T., Hutchings, G.J., Taylor, S.H. and Makkee, M. 2009. TAP reactor study of the deep oxidation of propane using cobalt oxide and gold-containing cobalt oxide catalysts. *Appl. Catal., A.* 365, 222-230.

Solsona, B.E., Garcia, T., Jones, C., Taylor, S.H., Carley, A.F. and Hutchings, G.J. 2006. Supported gold catalysts for the total oxidation of alkanes and carbon monoxide. *Appl. Catal., A.* 312, 67-76.

Song, W. and Hensen, E.J.M. 2013. Structure Sensitivity in CO Oxidation by a Single Au Atom Supported on Ceria. *J. Phys. Chem. C.* 117, 7721-7726.

Song, W., Perez Ferrandez, D.M., van Haandel, L., Liu, P., Nijhuis, T.A. and Hensen, E.J. 2015. Selective propylene oxidation to acrolein by gold dispersed on MgCuCr₂O₄ spinel. *ACS Catal.* 5, 1100-1111.

Srivastava, S.K., Yamada, R., Ogino, C. and Kondo, A. 2013. Biogenic synthesis and characterization of gold nanoparticles by Escherichia coli K12 and its heterogeneous catalysis in degradation of 4-nitrophenol. *Nanoscale Res. Lett.* 8, 70.

Sun, L., Sun, X., Zheng, Y., Lin, Q., Su, H. and Qi, C. 2017. Fabrication and characterization of core-shell polystyrene/polyaniline/Au composites and their catalytic properties for the reduction of 4-nitrophenol. *Synth. Met.* 224, 1-6.

Tai, Y., Murakami, J., Tajiri, K., Ohashi, F., Dat é M. and Tsubota, S. 2004. Oxidation of carbon monoxide on Au nanoparticles in titania and titania-coated silica aerogels. *Appl. Catal., A.* 268, 183-187.

Tai, Y. and Tajiri, K. 2008. Preparation, thermal stability, and CO oxidation activity of highly loaded Au/titania-coated silica aerogel catalysts. *Appl. Catal., A.* 342, 113-118.

Tai, Y., Watanabe, M., Kaneko, K., Tanemura, S., Miki, T., Murakami, J. and Tajiri, K. 2001. Preparation of Gold Cluster/Silica Nanocomposite Aerogel via Spontaneous Wet-Gel Formation. *Adv. Mater.* 13, 1611-1614.

Tamiolakis, I., Fountoulaki, S., Vordos, N., Lykakis, I.N. and Armatas, G.S. 2013. Mesoporous Au–TiO₂ nanoparticle assemblies as efficient catalysts for the chemoselective reduction of nitro compounds. *J. Mater. Chem. A.* 1, 14311-14319.

Tan, X., Liu, Y., Zeng, G., Wang, X., Hu, X., Gu, Y. and Yang, Z. 2015. Application of biochar for the removal of pollutants from aqueous solutions. *Chemosphere* 125, 70-85.

- Tang, W.-W., Zeng, G.-M., Gong, J.-L., Liang, J., Xu, P., Zhang, C. and Huang, B.-B. 2014. Impact of humic/fulvic acid on the removal of heavy metals from aqueous solutions using nanomaterials: A review. *Sci. Total Environ.* 468, 1014-1027.
- Torres, C.C., Alderete, J.B., Pecchi, G., Campos, C.H., Reyes, P., Pawelec, B., Vaschetto, E.G. and Eimer, G.A. 2016. Heterogeneous hydrogenation of nitroaromatic compounds on gold catalysts: Influence of titanium substitution in MCM-41 mesoporous supports. *Appl. Catal., A* 517, 110-119.
- Tsubota, S., Haruta, M., Kobayashi, T., Ueda, A. and Nakahara, Y. 1991 *Preparation of Catalysis V*, Elsevier, Amsterdam.
- Tuo, Y., Liu, G., Dong, B., Zhou, J., Wang, A., Wang, J., Jin, R., Lv, H., Dou, Z. and Huang, W. 2015. Microbial synthesis of Pd/Fe(3)O(4), Au/Fe(3)O(4) and PdAu/Fe(3)O(4) nanocomposites for catalytic reduction of nitroaromatic compounds. *Sci. Rep.* 5, 13515.
- Ulrich, V., Moroz, B., Sinev, I., Pyriaev, P., Bukhtiyarov, V. and Gr ünert, W. 2017. Studies on three-way catalysis with supported gold catalysts. Influence of support and water content in feed. *Appl. Catal., B* 203, 572-581.
- Varma, R.S. 2016. Greener and Sustainable Trends in Synthesis of Organics and Nanomaterials. *ACS Sustain. Chem. Eng.* 4, 5866-5878.
- Vidyasagar, D., Ghugal, S.G., Kulkarni, A., Mishra, P., Shende, A.G., Jagannath, Umare, S.S. and Sasikala, R. 2018. Silver/Silver(II) oxide (Ag/AgO) loaded graphitic carbon nitride microspheres: An effective visible light active photocatalyst for degradation of acidic dyes and bacterial inactivation. *Appl. Catal., B* 221, 339-348.
- Wain, A.J. 2013. Imaging size effects on the electrocatalytic activity of gold nanoparticles using scanning electrochemical microscopy. *Electrochim. Acta* 92, 383-391.
- Wang, C., Zou, W., Wang, J., Ge, Y., Lu, R. and Zhang, S. 2017a. Insight into the mechanism of gold-catalyzed reduction of nitroarenes based on the substituent effect and in situ IR. *New J. Chem.* 41, 3865-3871.
- Wang, D., Huang, L., Guo, Z., Han, X., Liu, C., Wang, W. and Yuan, W. 2018a. Enhanced photocatalytic hydrogen production over Au/SiC for water reduction by localized surface plasmon resonance effect. *Appl. Surf. Sci.* 456, 871-875.
- Wang, G.-H., Hilgert, J., Richter, F.H., Wang, F., Bongard, H.-J., Spliethoff, B., Weidenthaler, C. and Sch üth, F. 2014. Platinum–cobalt bimetallic nanoparticles in hollow carbon nanospheres for hydrogenolysis of 5-hydroxymethylfurfural. *Nat. Mater.* 13, 293.
- Wang, J., Shi, W., Liu, D., Zhang, Z., Zhu, Y. and Wang, D. 2017b. Supramolecular organic nanofibers with highly efficient and stable visible light photooxidation performance. *Appl. Catal., B* 202, 289-297.
- Wang, L., Guan, E., Zhang, J., Yang, J., Zhu, Y., Han, Y., Yang, M., Cen, C., Fu, G. and Gates, B.C. 2018b. Single-site catalyst promoters accelerate metal-catalyzed nitroarene hydrogenation. *Nat. commun.* 9, 1362.
- Wang, L., Jiang, X., Zhang, M., Yang, M. and Liu, Y.-N. 2017c. In Situ Assembly of Au

- Nanoclusters within Protein Hydrogel Networks. *Chem-Asian J.* 12, 2374-2378.
- Wang, L., Wang, H., Rice, A.E., Zhang, W., Li, X., Chen, M., Meng, X., Lewis, J.P. and Xiao, F.-S. 2015a. Design and Preparation of Supported Au Catalyst with Enhanced Catalytic Activities by Rationally Positioning Au Nanoparticles on Anatase. *J. Phys. Chem. Lett.* 6, 2345-2349.
- Wang, L., Zhang, J., Wang, H., Shao, Y., Liu, X., Wang, Y.-Q., Lewis, J.P. and Xiao, F.-S. 2016. Activity and Selectivity in Nitroarene Hydrogenation over Au Nanoparticles on the Edge/Corner of Anatase. *ACS Catal.* 6, 4110-4116.
- Wang, S., Wang, J., Zhao, Q., Li, D., Wang, J.-Q., Cho, M., Cho, H., Terasaki, O., Chen, S. and Wan, Y. 2015b. Highly active heterogeneous 3 nm gold nanoparticles on mesoporous carbon as catalysts for low-temperature selective oxidation and reduction in water. *ACS Catal.* 5, 797-802.
- Wang, S., Zhao, Q., Wei, H., Wang, J.-Q., Cho, M., Cho, H.S., Terasaki, O. and Wan, Y. 2013. Aggregation-free gold nanoparticles in ordered mesoporous carbons: toward highly active and stable heterogeneous catalysts. *JACS* 135, 11849-11860.
- Wang, T., Yao, Y., Wei, A., Jia, L. and Chen, S. 2018c. Facile synthesis, microstructure, and photocatalytic activity of novel flower-like apatite@Au composite nanosheet spheres. *Mater. Lett.* 220, 129-132.
- Wang, Y., Wei, G., Zhang, W., Jiang, X., Zheng, P., Shi, L. and Dong, A. 2007. Responsive catalysis of thermoresponsive micelle-supported gold nanoparticles. *J. Mol. Catal. A: Chem.* 266, 233-238.
- Waters, R.D., Weimer, J.J. and Smith, J.E. 1994. An investigation of the activity of coprecipitated gold catalysts for methane oxidation. *Catal. Lett.* 30, 181-188.
- Wei, Y., Zhou, H., Zhang, H., Zhu, X., Liu, G., Li, Y. and Cai, W. 2017a. One - Step and Surfactant - Free Fabrication of Gold - Nanoparticle - Decorated Bismuth Oxychloride Nanosheets Based on Laser Ablation in Solution and Their Enhanced Visible - Light Plasmonic Photocatalysis. *ChemPhysChem* 18, 1146-1154.
- Wei, Z., Rosa, L., Wang, K., Endo, M., Juodkazis, S., Ohtani, B. and Kowalska, E. 2017b. Size-controlled gold nanoparticles on octahedral anatase particles as efficient plasmonic photocatalyst. *Appl. Catal., B.* 206, 393-405.
- Wu, H., Lai, C., Zeng, G., Liang, J., Chen, J., Xu, J., Dai, J., Li, X., Liu, J. and Chen, M. 2017. The interactions of composting and biochar and their implications for soil amendment and pollution remediation: a review. *Crit. Rev. Biotechnol.* 37, 754-764.
- Wu, H., Liu, Z., Wang, X., Zhao, B., Zhang, J. and Li, C. 2006. Preparation of hollow capsule-stabilized gold nanoparticles through the encapsulation of the dendrimer. *J. Colloid Interface Sci.* 302, 142-148.
- Wu, L., Li, F., Xu, Y., Zhang, J.W., Zhang, D., Li, G. and Li, H. 2015a. Plasmon-induced photoelectrocatalytic activity of Au nanoparticles enhanced TiO₂ nanotube arrays electrodes for environmental remediation. *Appl. Catal., B.* 164, 217-224.
- Wu, T., Zhang, L., Gao, J., Liu, Y., Gao, C. and Yan, J. 2013. Fabrication of graphene oxide decorated with Au-Ag alloy nanoparticles and its superior catalytic performance for the

- reduction of 4-nitrophenol. *J. Mater. Chem. A*. 1, 7384-7390.
- Wu, X.-Q., Wu, X.-W., Huang, Q., Shen, J.-S. and Zhang, H.-W. 2015b. In situ synthesized gold nanoparticles in hydrogels for catalytic reduction of nitroaromatic compounds. *Appl. Surf. Sci.* 331, 210-218.
- Wunder, S., Lu, Y., Albrecht, M. and Ballauff, M. 2011. Catalytic Activity of Faceted Gold Nanoparticles Studied by a Model Reaction: Evidence for Substrate-Induced Surface Restructuring. *ACS Catal.* 1, 908-916.
- Wunder, S., Polzer, F., Lu, Y., Mei, Y. and Ballauff, M. 2010. Kinetic Analysis of Catalytic Reduction of 4-Nitrophenol by Metallic Nanoparticles Immobilized in Spherical Polyelectrolyte Brushes. *J. Phys. Chem. C*. 114, 8814-8820.
- Xia, J., He, G., Zhang, L., Sun, X. and Wang, X. 2016. Hydrogenation of nitrophenols catalyzed by carbon black-supported nickel nanoparticles under mild conditions. *Appl. Catal., B*. 180, 408-415.
- Xia, J., Zhang, L., Fu, Y., He, G., Sun, X. and Wang, X. 2018. Nitrogen-doped carbon black supported NiCo₂S₄ catalyst for hydrogenation of nitrophenols under mild conditions. *J. Mater. Sci.* 53, 4467-4481.
- Xiang, S., Zhang, Y., Zhou, Y., Zhang, Z., Sheng, X. and Xu, Y. 2014. Synthesis and characterization of carbon nanotubes supported Au nanoparticles encapsulated in various oxide shells. *RSC Adv.* 4, 51334-51341.
- Xiao, Q., Sarina, S., Waclawik, E.R., Jia, J., Chang, J., Riches, J.D., Wu, H., Zheng, Z. and Zhu, H. 2016. Alloying Gold with Copper Makes for a Highly Selective Visible-Light Photocatalyst for the Reduction of Nitroaromatics to Anilines. *ACS Catal.* 6, 1744-1753.
- Xie, T., Zhao, X., Zhang, J., Shi, L. and Zhang, D. 2015. Ni nanoparticles immobilized Ce-modified mesoporous silica via a novel sublimation-deposition strategy for catalytic reforming of methane with carbon dioxide. *Int. J. Hydrogen Energy* 40, 9685-9695.
- Xing, Z.-M., Gao, Y.-X., Shi, L.-Y., Liu, X.-Q., Jiang, Y. and Sun, L.-B. 2017. Fabrication of gold nanoparticles in confined spaces using solid-phase reduction: Significant enhancement of dispersion degree and catalytic activity. *Chem. Eng. Sci.* 158, 216-226.
- Xu, P., Zeng, G.M., Huang, D.L., Feng, C.L., Hu, S., Zhao, M.H., Lai, C., Wei, Z., Huang, C. and Xie, G.X. 2012a. Use of iron oxide nanomaterials in wastewater treatment: a review. *Sci. Total Environ.* 424, 1-10.
- Xu, P., Zeng, G.M., Huang, D.L., Lai, C., Zhao, M.H., Wei, Z., Li, N.J., Huang, C. and Xie, G.X. 2012b. Adsorption of Pb (II) by iron oxide nanoparticles immobilized *Phanerochaete chrysosporium*: equilibrium, kinetic, thermodynamic and mechanisms analysis. *Chem. Eng. J.* 203, 423-431.
- Xu, X., Duan, G., Li, Y., Liu, G., Wang, J., Zhang, H., Dai, Z. and Cai, W. 2014. Fabrication of Gold Nanoparticles by Laser Ablation in Liquid and Their Application for Simultaneous Electrochemical Detection of Cd²⁺, Pb²⁺, Cu²⁺, Hg²⁺. *ACS Appl. Mater. Interfaces* 6, 65-71.
- Xue, W., Huang, D., Zeng, G., Wan, J., Zhang, C., Xu, R., Cheng, M. and Deng, R. 2018. Nanoscale

- zero-valent iron coated with rhamnolipid as an effective stabilizer for immobilization of Cd and Pb in river sediments. *J. Hazard. Mater.* 341, 381-389.
- Yang, C., Chen, H., Zeng, G., Yu, G. and Luo, S. 2010. Biomass accumulation and control strategies in gas biofiltration. *Biotechnol. Adv.* 28, 531-540.
- Yang, F., Chen, M. and Goodman, D. 2008. Sintering of Au particles supported on TiO₂ (110) during CO oxidation. *J. Phys. Chem. C* 113, 254-260.
- Yang, K., Huang, K., He, Z., Chen, X., Fu, X. and Dai, W. 2014a. Promoted effect of PANI as electron transfer promoter on CO oxidation over Au/TiO₂. *Appl. Catal., B* 158-159, 250-257.
- Yang, K., Huang, K., Lin, L., Chen, X., Dai, W. and Fu, X. 2015. Superior preferential oxidation of carbon monoxide in hydrogen-rich stream under visible light irradiation over gold loaded hedgehog-shaped titanium dioxide nanospheres: Identification of copper oxide decoration as an efficient promoter. *J. Power Sources* 284, 194-205.
- Yang, K., Liu, J., Si, R., Chen, X., Dai, W. and Fu, X. 2014b. Comparative study of Au/TiO₂ and Au/Al₂O₃ for oxidizing CO in the presence of H₂ under visible light irradiation. *J. Catal.* 317, 229-239.
- Yang, K., Meng, C., Lin, L., Peng, X., Chen, X., Wang, X., Dai, W. and Fu, X. 2016a. A heterostructured TiO₂-C₃N₄ support for gold catalysts: a superior preferential oxidation of CO in the presence of H₂ under visible light irradiation and without visible light irradiation. *Catal. Sci. Technol.* 6, 829-839.
- Yang, K., Zhang, Y., Li, Y., Huang, P., Chen, X., Dai, W. and Fu, X. 2016b. Insight into the function of alkaline earth metal oxides as electron promoters for Au/TiO₂ catalysts used in CO oxidation. *Appl. Catal., B* 183, 206-215.
- Yang, X., Tian, P.-F., Zhang, C., Deng, Y.-q., Xu, J., Gong, J. and Han, Y.-F. 2013. Au/carbon as Fenton-like catalysts for the oxidative degradation of bisphenol A. *Appl. Catal., B* 134-135, 145-152.
- Ye, W., Yu, J., Zhou, Y., Gao, D., Wang, D., Wang, C. and Xue, D. 2016. Green synthesis of Pt-Au dendrimer-like nanoparticles supported on polydopamine-functionalized graphene and their high performance toward 4- nitrophenol reduction. *Appl. Catal., B* 181, 371-378.
- Yi, H., Huang, D., Qin, L., Zeng, G., Lai, C., Cheng, M., Ye, S., Song, B., Ren, X. and Guo, X. 2018. Selective prepared carbon nanomaterials for advanced photocatalytic application in environmental pollutant treatment and hydrogen production. *Appl. Catal., B* 239, 408-424.
- Ying, C., Wen-Chao, P. and Xiao-Yan, L. 2017. Synthesis of MoS₂/graphene hybrid supported Au and Ag nanoparticles with multi-functional catalytic properties. *Nanotechnology* 28, 205603.
- Yu, H., Chen, M., Rice, P.M., Wang, S.X., White, R. and Sun, S. 2005. Dumbbell-like bifunctional Au- Fe₃O₄ nanoparticles. *Nano Lett.* 5, 379-382.
- Zeng, G., Zhang, C., Huang, D., Lai, C., Tang, L., Zhou, Y., Xu, P., Wang, H., Qin, L. and Cheng, M. 2017. Practical and regenerable electrochemical aptasensor based on nanoporous gold and thymine-Hg²⁺-thymine base pairs for Hg²⁺ detection. *Biosens. Bioelectron.* 90, 542-548.
- Zeng, J., Zhang, Q., Chen, J. and Xia, Y. 2009. A comparison study of the catalytic properties of

- Au-based nanocages, nanoboxes, and nanoparticles. *Nano Lett.* 10, 30-35.
- Zeng, T., Zhang, X.-l., Niu, H.-y., Ma, Y.-r., Li, W.-h. and Cai, Y.-q. 2013. In situ growth of gold nanoparticles onto polydopamine-encapsulated magnetic microspheres for catalytic reduction of nitrobenzene. *Appl. Catal., B.* 134, 26-33.
- Zhang, C., Lai, C., Zeng, G., Huang, D., Yang, C., Wang, Y., Zhou, Y. and Cheng, M. 2016. Efficacy of carbonaceous nanocomposites for sorbing ionizable antibiotic sulfamethazine from aqueous solution. *Water Res.* 95, 103-112.
- Zhang, C., Liu, L., Zeng, G.-M., Huang, D.-L., Lai, C., Huang, C., Wei, Z., Li, N.-J., Xu, P. and Cheng, M. 2014a. Utilization of nano-gold tracing technique: Study the adsorption and transmission of laccase in mediator-involved enzymatic degradation of lignin during solid-state fermentation. *Biochem. Eng. J.* 91, 149-156.
- Zhang, J., Chen, G., Guay, D., Chaker, M. and Ma, D. 2014b. Highly active PtAu alloy nanoparticle catalysts for the reduction of 4-nitrophenol. *Nanoscale* 6, 2125-2130.
- Zhang, P., Shao, C., Li, X., Zhang, M., Zhang, X., Su, C., Lu, N., Wang, K. and Liu, Y. 2013. An electron-rich free-standing carbon@ Au core-shell nanofiber network as a highly active and recyclable catalyst for the reduction of 4-nitrophenol. *Phys. Chem. Chem. Phys.* 15, 10453-10458.
- Zhang, P., Shao, C., Zhang, Z., Zhang, M., Mu, J., Guo, Z. and Liu, Y. 2011a. TiO₂@ carbon core/shell nanofibers: controllable preparation and enhanced visible photocatalytic properties. *Nanoscale* 3, 2943-2949.
- Zhang, Y., Li, Q., Liu, C., Shan, X., Chen, X., Dai, W. and Fu, X. 2018. The promoted effect of a metal-organic frameworks (ZIF-8) on Au/TiO₂ for CO oxidation at room temperature both in dark and under visible light irradiation. *Appl. Catal., B.* 224, 283-294.
- Zhang, Y., Zeng, G.M., Tang, L., Chen, J., Zhu, Y., He, X.X. and He, Y. 2015. Electrochemical sensor based on electrodeposited graphene-Au modified electrode and nanoAu carrier amplified signal strategy for attomolar mercury detection. *Anal. Chem.* 87, 989-996.
- Zhang, Z., Shao, C., Zou, P., Zhang, P., Zhang, M., Mu, J., Guo, Z., Li, X., Wang, C. and Liu, Y. 2011b. In situ assembly of well-dispersed gold nanoparticles on electrospun silica nanotubes for catalytic reduction of 4-nitrophenol. *Chem. Commun.* 47, 3906-3908.
- Zhao, M., Yuan, K., Wang, Y., Li, G., Guo, J., Gu, L., Hu, W., Zhao, H. and Tang, Z. 2016a. Metal-organic frameworks as selectivity regulators for hydrogenation reactions. *Nature* 539, 76.
- Zhao, P., Feng, X., Huang, D., Yang, G. and Astruc, D. 2015. Basic concepts and recent advances in nitrophenol reduction by gold- and other transition metal nanoparticles. *Coord. Chem. Rev.* 287, 114-136.
- Zhao, X., Li, H., Zhang, J., Shi, L. and Zhang, D. 2016b. Design and synthesis of NiCe@m-SiO₂ yolk-shell framework catalysts with improved coke- and sintering-resistance in dry reforming of methane. *Int. J. Hydrogen Energy* 41, 2447-2456.
- Zheng, J., Dong, Y., Wang, W., Ma, Y., Hu, J., Chen, X. and Chen, X. 2013. In situ loading of gold nanoparticles on Fe₃O₄@SiO₂ magnetic nanocomposites and their high catalytic activity.

1666 Nanoscale 5, 4894-4901.

1667 Zheng, N. and Stucky, G.D. 2006. A General Synthetic Strategy for Oxide-Supported Metal
1668 Nanoparticle Catalysts. JACS 128, 14278-14280.

1669 Zheng, Q., Durkin, D.P., Elenewski, J.E., Sun, Y., Banek, N.A., Hua, L., Chen, H., Wagner, M.J.,
1670 Zhang, W. and Shuai, D. 2016. Visible-light-responsive graphitic carbon nitride: rational design
1671 and photocatalytic applications for water treatment. Environ. Sci. Technol. 50, 12938-12948.

1672 Zhong, R.-Y., Yan, X.-H., Gao, Z.-K., Zhang, R.-J. and Xu, B.-Q. 2013. Stabilizer substitution and
1673 its effect on the hydrogenation catalysis by Au nanoparticles from colloidal synthesis. Catal. Sci.
1674 Technol. 3, 3013-3019.

1675 Zhong, Y., Li, T., Lin, H., Zhang, L., Xiong, Z., Fang, Q., Zhang, G. and Liu, F. 2018. Meso-/macro-
1676 porous microspheres confining Au nanoparticles based on PDLA/PLLA stereo-complex
1677 membrane for continuous flowing catalysis and separation. Chem. Eng. J. 344, 299-310.

1678 Zhou, C., Lai, C., Huang, D., Zeng, G., Zhang, C., Cheng, M., Hu, L., Wan, J., Xiong, W., Wen, M.,
1679 Wen, X. and Qin, L. 2018a. Highly porous carbon nitride by supramolecular preassembly of
1680 monomers for photocatalytic removal of sulfamethazine under visible light driven. Appl. Catal.,
1681 B. 220, 202-210.

1682 Zhou, X., Lai, C., Huang, D., Zeng, G., Chen, L., Qin, L., Xu, P., Cheng, M., Huang, C., Zhang, C.
1683 and Zhou, C. 2018b. Preparation of water-compatible molecularly imprinted thiol-
1684 functionalized activated titanium dioxide: Selective adsorption and efficient photodegradation
1685 of 2, 4-dinitrophenol in aqueous solution. J. Hazard. Mater. 346, 113-123.

1686 Zhu, N., Cao, Y., Shi, C., Wu, P. and Ma, H. 2016. Biorecovery of gold as nanoparticles and its
1687 catalytic activities for p-nitrophenol degradation. Environmental Science and Pollution
1688 Research 23, 7627-7638.

1689 Zinchenko, A., Miwa, Y., Lopatina, L.I., Sergeyev, V.G. and Murata, S. 2014. DNA Hydrogel as a
1690 Template for Synthesis of Ultrasmall Gold Nanoparticles for Catalytic Applications. ACS Appl.
1691 Mater. Interfaces 6, 3226-3232.

Figure Captions

Fig. 1 Langmuir–Hinshelwood model for reduction of 4-NP by Au/Pt NPs catalysis.

Adapted with permission from ref.(Wunder et al. 2010) Copyright 2010 the American Chemical Society.

Fig. 2. Mechanism illustration for direct and condensation route of nitroaromatics reduction by Au nanocatalysts and H₂.

Fig. 3 Reaction mechanism for reduction of nitroarene by (NAP)-Mg–Au(0) catalyst.

Adapted with permission from ref. (Layek et al. 2012) Copyright 2012 the Royal Society of Chemistry.

Fig. 4 Mechanism illustration for reduction of 4-NP under the illumination of light.

Adapted with permission from ref. (Koklioti et al. 2017) Copyright 2012 the Royal Society of Chemistry.

Fig. 5. Mechanism for reduction of 4-NP raspberry-like polymer supported Au nanocatalyst. Adapted with permission from ref.(Li and Chen 2013) Copyright 2013 the Royal Society of Chemistry.

Fig. 6 Illustration of SiO₂ supported AuNPs for nitroaromatics reduction. (A) Core-shell structure of encapsulating one or many AuNP; (B) AuNPs are deposited on the inside or outside the surface of SiO₂ nanotubes; (C) AuNPs are half-embedded or combined on the surface of SiO₂ microsphere.

Fig. 7 Synthetic process of (A) calcine reduced AuCS and (B) grind formed AuAS catalysts. Adapted with permission from ref.(Xing et al. 2017) Copyright 2017 Elsevier.

Fig. 8 Mechanism of (A) preparation process and (B) formation mechanism of raspberry-like Au/SiO₂ nanocomposite particles. Adapted with permission from

ref.(Cao et al. 2016) Copyright 2016 Elsevier.

Fig. 9. Absorption of nitrobenzene on TiO₂ supported Au nanocatalyst with oxygen vacancies. Adapted with permission from ref.(Wang et al. 2016) Copyright 2016 the American Chemical Society.

Fig. 10. Enhanced activity and selectivity for nitrobenzene reduction by Sn decorated M/TiO₂ catalyst. Adapted with permission from ref.(Wang et al. 2018b) Copyright 2018 Nature.

Fig. 11. Photographic representation for (A) preparation of Fe₃O₄-SiO₂ magnetic nanospheres supported Au nanocatalyst and (B) in reduction of 4-NP using NaBH₄. Adapted with permission from ref.(Zheng et al. 2013) Copyright 2013 The Royal Society of Chemistry.

Fig. 12. 4-NP reduction process (a) in the dark, (b) under visible light and (c) solar light illumination. Adapted with permission from ref. (Liu et al. 2017b) Copyright 2017 Elsevier.

Fig. 13. Schematic for (A) fabrication, (B) SEM image, and (C) TEM image of Fe₃O₄@TiO₂@Ag-Au microspheres. Adapted with permission from ref.(Shen et al. 2017a) Copyright 2017 Elsevier.

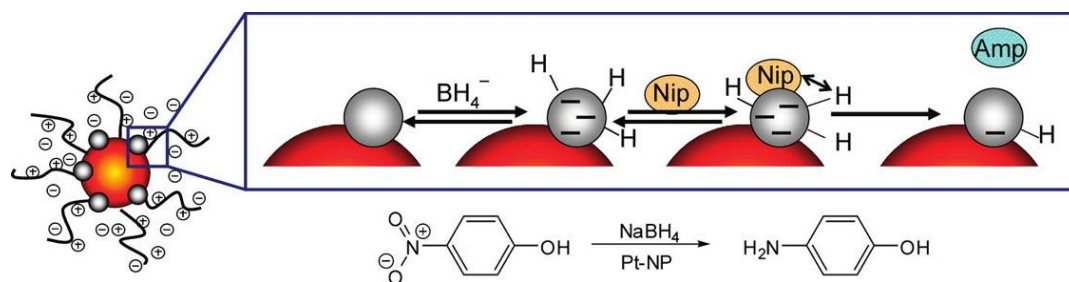
Fig. 14. Figures and TEM images of Au nanocrystals with different shapes. (A) Polyhedral and nanorods; Adapted with permission from ref.(Premkumar et al. 2011) Copyright 2011 Springer. (B) flowers; Adapted with permission from ref.(Liu et al. 2017a) Copyright 2017 Elsevier. (C) cages; (D) boxes; Adapted with permission from ref.(Zeng et al. 2009) Copyright 2010 the American Chemical Society. (E) stars.

1737 Adapted with permission from ref.(Ma et al. 2017) Copyright 2017 Multidisciplinary

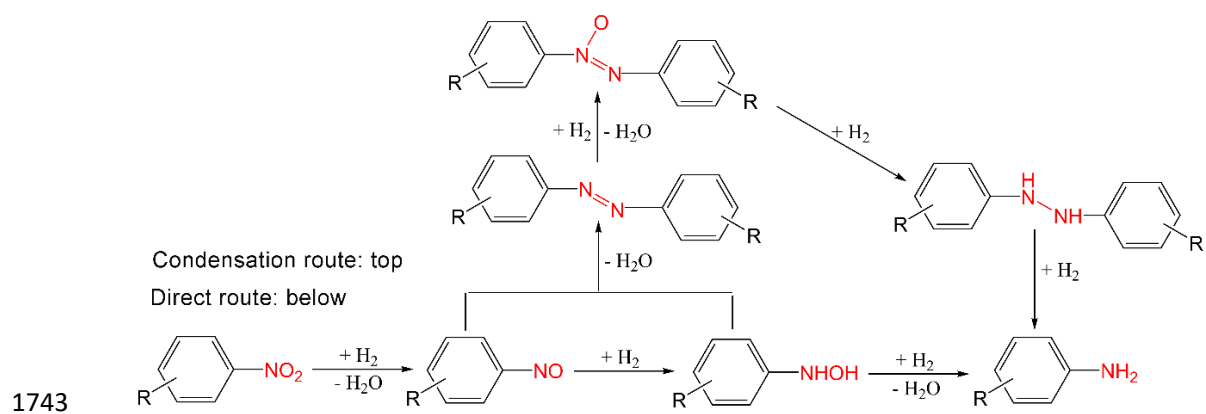
1738 Digital Publishing Institute.

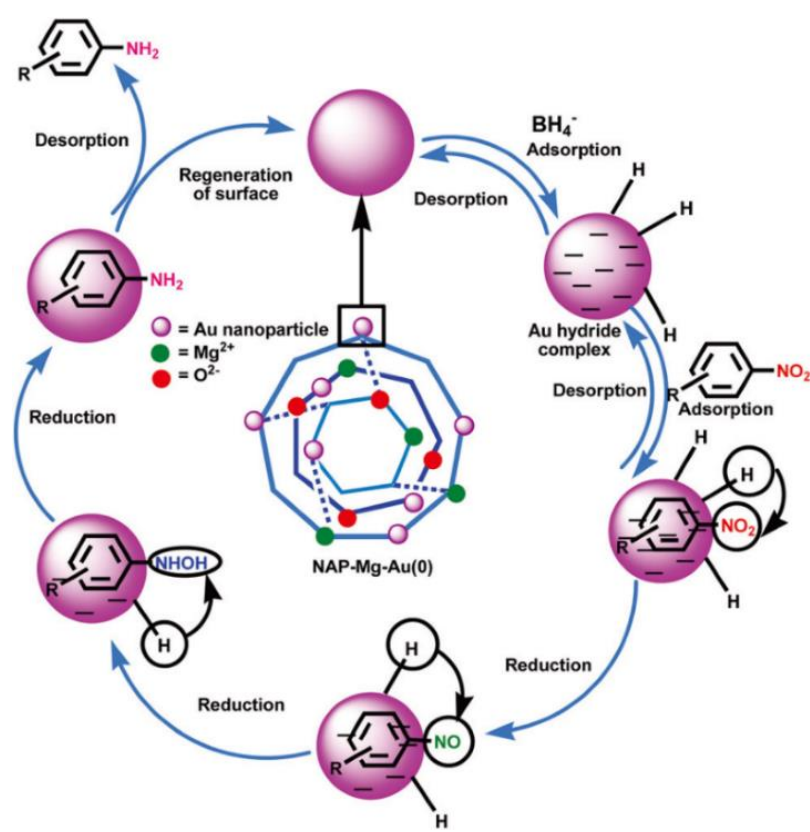
Figures

Fig. 1

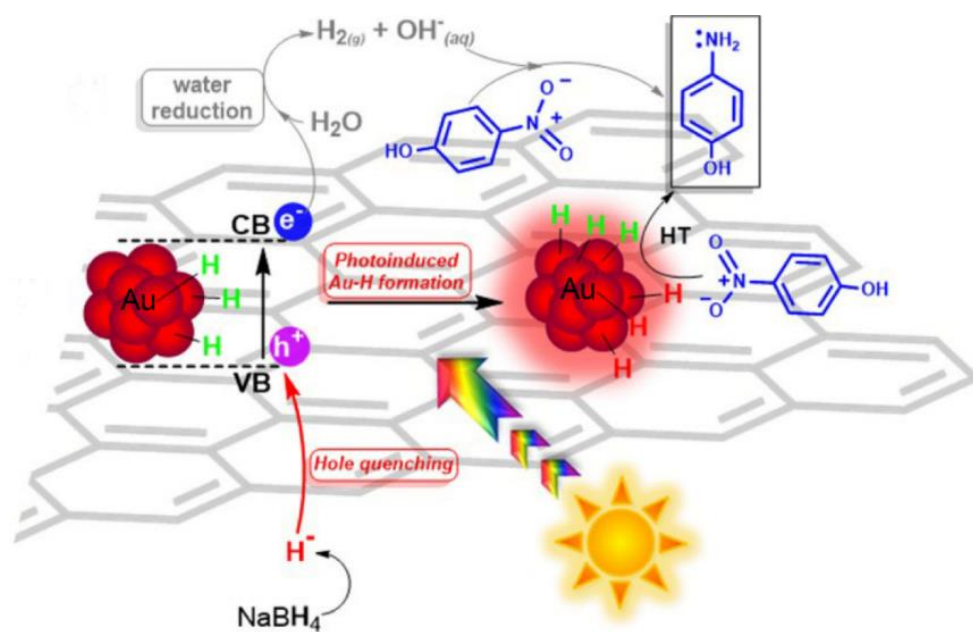


1742 **Fig. 2**



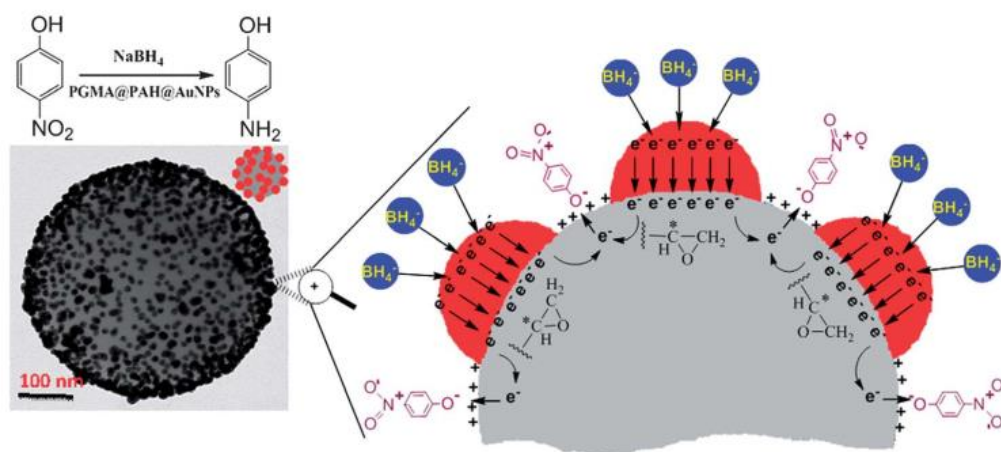


1746 **Fig. 4**

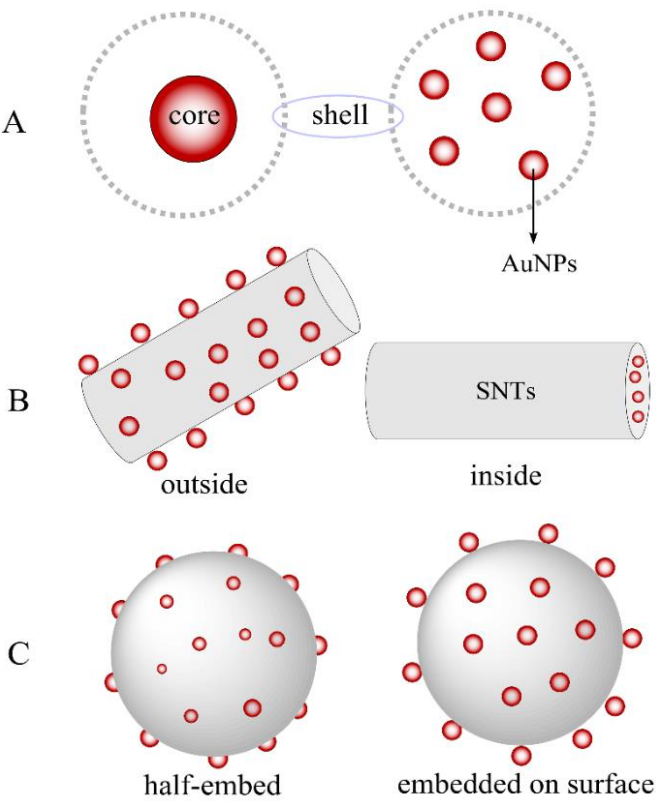


1747

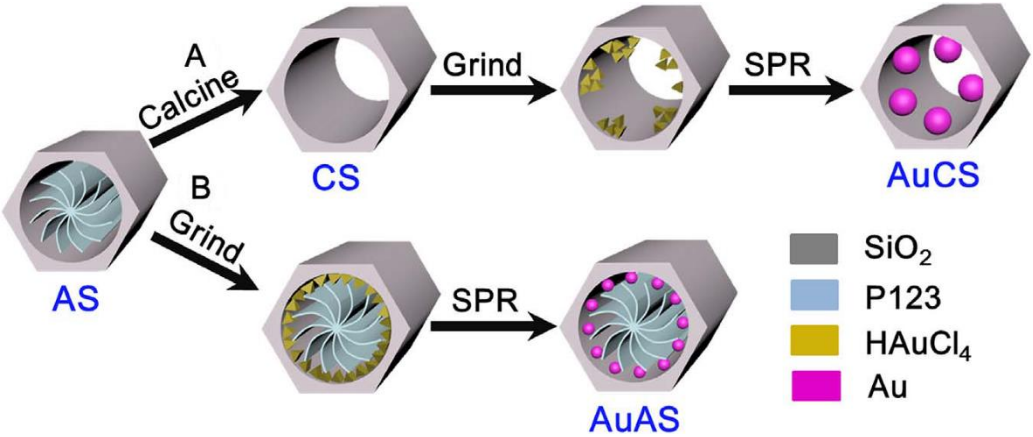
1748 **Fig. 5**



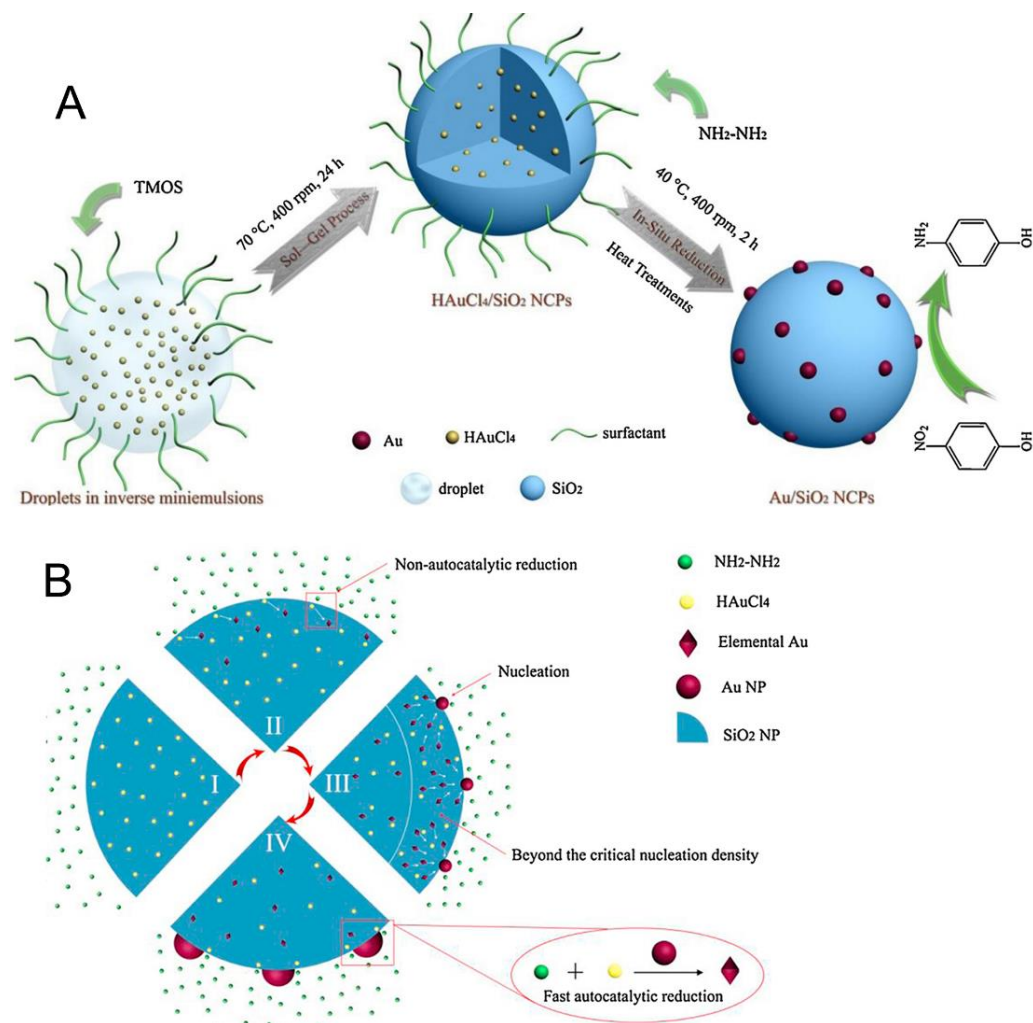
1749



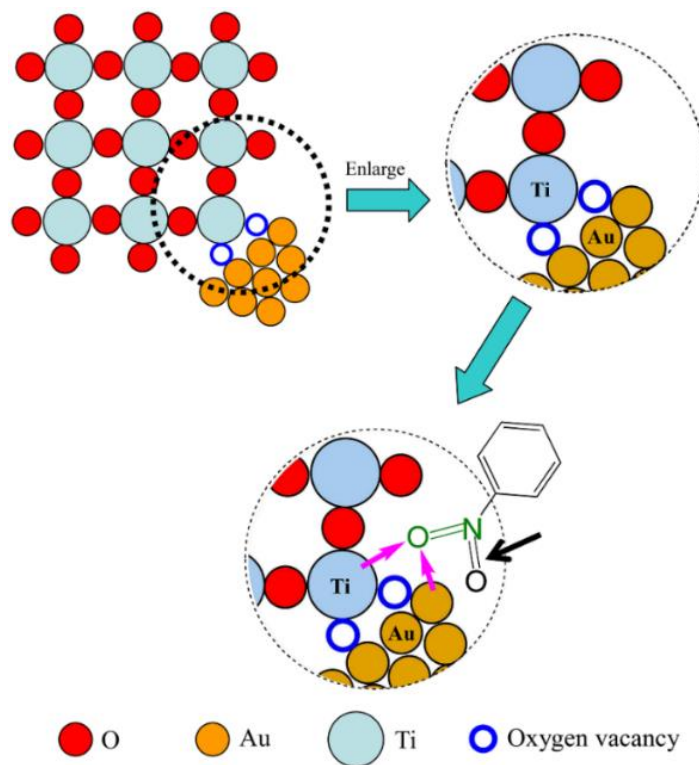
1752 **Fig. 7**



1753

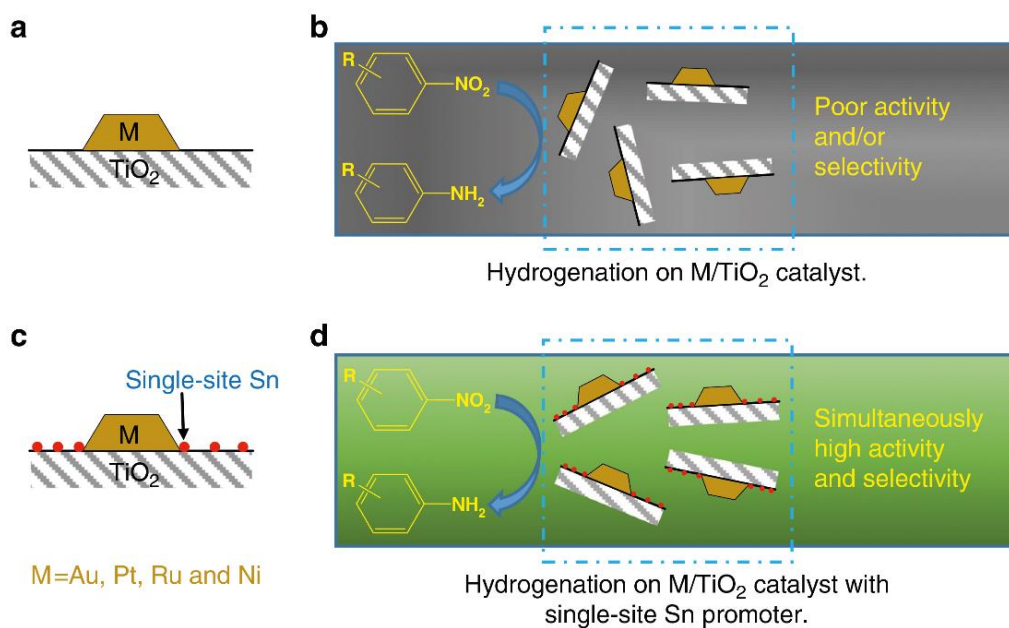


1756 **Fig. 9**



1757

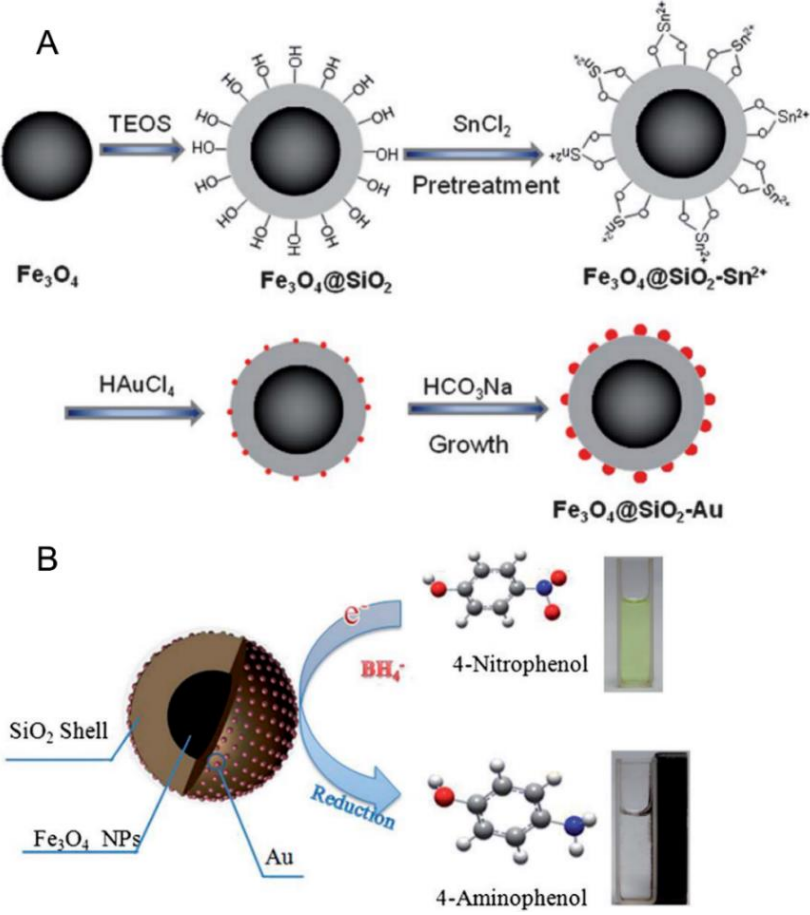
1758 **Fig. 10**



1759

1760

1761 **Fig. 11**



1762

1763

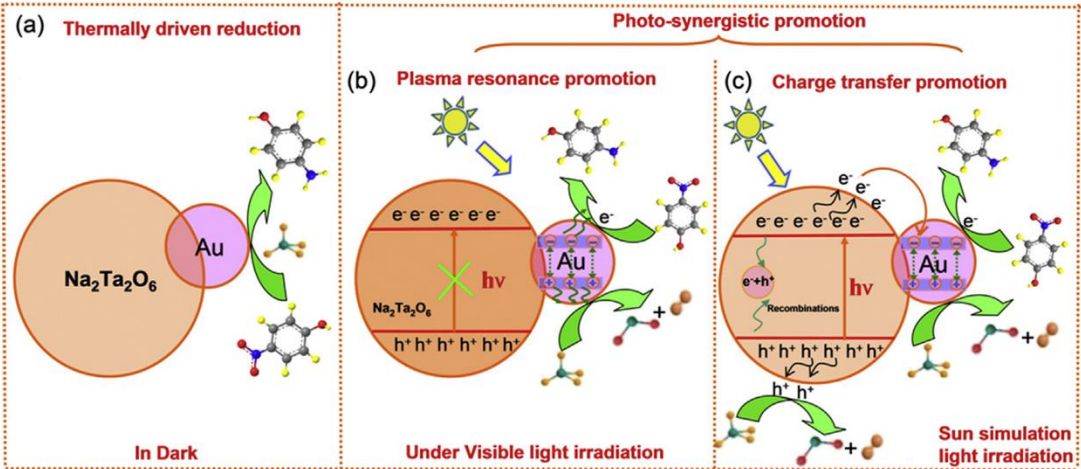
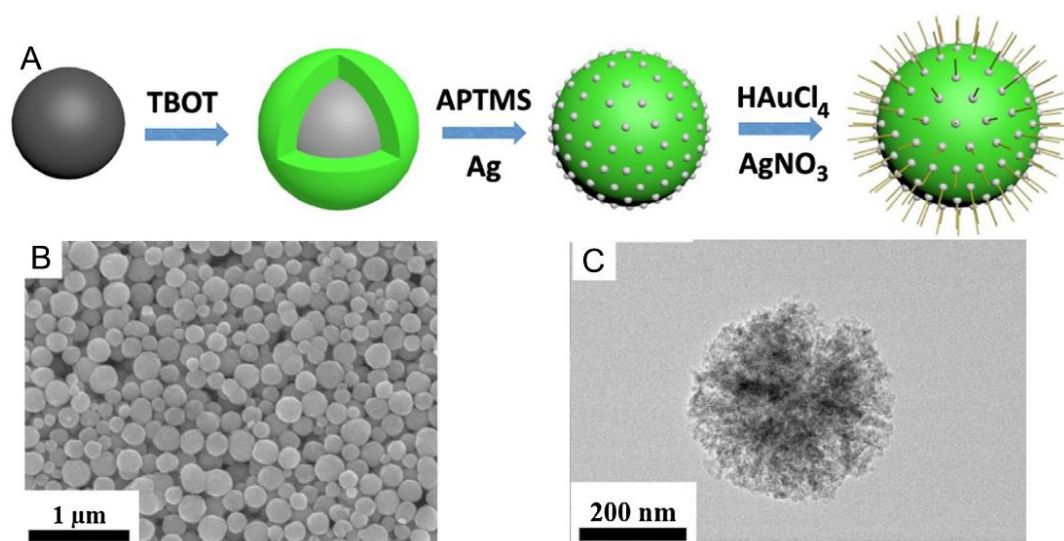
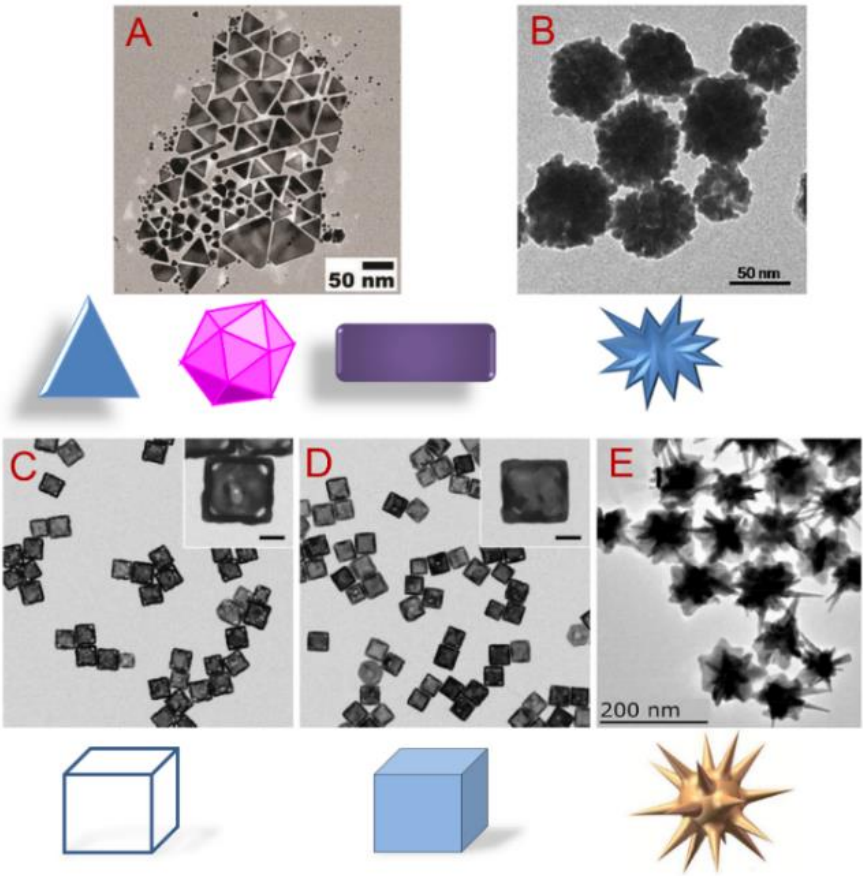


Fig. 13



1769 **Fig. 14**



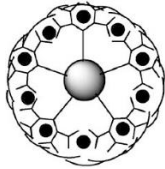
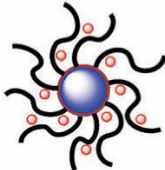
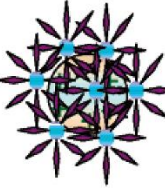
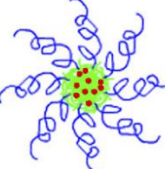
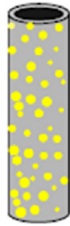
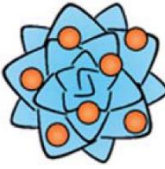
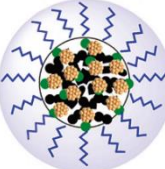
1770

1771

1773 **Table 1** Comparison of some typical strategies for reduction of 4-NP using free AuNPs

Type of composition	Composition	Particle size (nm)	k_{app} (min^{-1})	Concentration of catalyst (mM)	k_{nor} ($\text{min}^{-1} \text{mM}^{-1}$)	Ref.
Bacteria stabilized AuNPs	Breynia rhamnoides	25	0.552	-	-	(Gangula et al. 2011)
	<i>Escherichia Coli</i> bacterium	10	0.210	-	-	(Badwaik et al. 2011)
	Escherichia coli K12	50	0.014	0.0042	3.33	(Srivastava et al. 2013)
	Shewanella halotis	<10	0.654	0.005	130.8	(Zhu et al. 2016)
	Cylindrocladium floridanum	25	0.027	0.0051	5.29	(Narayanan and Sakthivel 2011)
Fungi	<i>Rhizopus oryzae</i> protein extract	5-65	2.60×10^6 - 4.99×10^5	0.0101	2.57×10^8 - 4.94×10^7	(Das et al. 2012)
	<i>Pycnoporus sanguineus</i>	6.07	0.066	0.019 mg	3.47 mg^{-1}	(Shi et al. 2015)
	<i>Fusarium</i> sp. MMT1 strain.	30.6	0.102	-	-	(Guria et al. 2016)
	<i>Trichosporon montevidense</i>	12	1.5	0.0015	1000	(Shen et al. 2016)
	<i>Aspergillus</i> sp. WL	4.4	9.8-25.2	0.58	16.9-43.45	(Shen et al. 2017b)
		28.4	10.6	3	3.53	(Qu et al. 2017)
Gel	DNA hydrogel	2-3	1.5	100 mg	0.015 mg^{-1}	(Zinchenko et al. 2014)
	Hydrogels	-	2.6	0.005	520	(Wu et al. 2015b)
Others	CTAB	13	6	0.25	24	(Fenger et al. 2012)
	Olibanum gum	3 \pm 4	5.8	-	-	(Guadie Assefa et al. 2017)
	dimethyl sulfoxide	15-40	5.4	-	-	(Bhosale et al. 2017)

Table 2 Different shapes of typical polymer-supported **Au nanocatalysts**.

Shape	Schematic	Preparation procedure	Particle size (nm)	Ref.
Dendrimer		i. Graft dendrimer on the surface of silica; ii. Reduce AuNPs on dendrimer-modified silica by NaBH ₄ ; iii. Self-assemble with polyelectrolytes and remove silica cores.	2.3 ± 0.8	(Wu et al. 2006)
Brush		i. Functionalize SiO ₂ NPs with APTES to provide amino groups; ii. Graft PDMAEMA onto them with SIPGP; iii. Reduce AuNPs onto the PDMAEMA brushes.	3.0	(Chen et al. 2014a)
Bead		i. Prepare AuNPs of different size using Frens method; ii. Immobilize prepared AuNPs into the resin beads.	20	(Pani grahi et al. 2007)
Micelle		i. Synthesize block copolymer by ATRP; ii. Prepare core-corona micelles and micelle supported-AuNPs by NaBH ₄ reduction.	2-4	(Wang et al. 2007)
Nanotube		i. Synthesize PPyNTs by a self-degraded template method and ILS/PPyNTs; ii. Reduce AuNPs on the ILS/PPyNTs and by NaBH ₄ to form Au/ ILS/PPyNTs hybrids and Au/PPyNTs hybrids.	5.7	(Qiu et al. 2012)
Flower		i. Prepare BP; ii. Synthesize hybrid BP-AuNPs by deposition reduction approach;	5.5 ± 1.7	(Matsushima et al. 2012)
Star		i. Synthesize MAOELP and microemulsion copolymerize inimer BIEM with it; ii. Prepare hyperstar polymer by polymerization; iii. Form HS-Au ₂₅ (SR) ₁₈ nanocomposites via ligand exchange.	-	(Hu et al. 2017)

APTES: 3-aminopropyltriethoxysilane; PDMAEMA: Poly(2-(dimethylamino) ethyl methacrylate);

1777 SIPGP: self-initiated photografting and photopolymerization; ATRP: atom transfer radical
1778 polymerization; PS-PBIEM: polystyrene- polymerizing 2-(2-bromoisobutyryloxy) ethylmethacrylate;
1779 PPyNTs: polypyrrole nanotubes; ILS: ionic liquids; BP: boronate microparticles; MAOELP: 2-
1780 methacryloyloxyethyl lipoate.

1781 **Table 3** Details of different parameters and reaction conditions of oxides-based Au

1782 nanocatalysts for 4-NP reduction

Catalyst type	Particle size (nm)	Amount of Au (μmol)	Amount of NaBH_4 (mmol)	Amount of 4-NP (μmol)	k_{app} (10^{-3} s^{-1})	Reaction time (min)	Recycle	Ref.
Au@SiO ₂	104-43	1.6	1.2	3400	14-3.9	60	-	(Lee et al. 2008)
Au@hm ^a -ZrO ₂	6.3	25	12000	6.8	5.17	12	4	(Huang et al. 2009)
AuNPs/SNTs	3-5	1	0.15	3.6	10.64	4.7	-	(Zhang et al. 2011b)
Au/SBA-15	2.5	0.133 g/L	0.4	30	17.42	4	5	(Miah et al. 2017)
AuAS	3.9	0.8 g/L	0.04	0.1	2.92	24	5	(Xing et al. 2017)
Au@meso-SiO ₂	2.5	0.05 mL 0.0125 wt%	0.025	0.0625	1.33	20	5	(Chen et al. 2014b)
Au/TiO ₂	-	1.5 g/L	0.036	0.6	2.83	20	-	(Li et al. 2015)
dumbbell-like Au-Fe ₃ O ₄	5	2 mg	0.016	0.4	10.5	5	6	(Lin and Doong 2011)
flower-like Au-Fe ₃ O ₄	10				6.33	6.67		
Fe ₃ O ₄ @SiO ₂ -Au MNCs ^b	5	0.5 mg	0.2	0.25	14.2	4	9	(Zheng et al. 2013)

1783 hm^a, hollow mesoporous; MNCs^b, magnetic nanocomposites

1784 **Table 4** Comparison of different carbon-supported **Au nanocatalysts** for reduction of
 1785 nitroaromatics

Catalyst	Nitroaromatics	Structure	Particle size (nm)	k_{app} (min^{-1})	k_{nor} ($\text{s}^{-1} \text{g}^{-1}$)	Ref.
USP Au/C	4-NP	Encapsulated	33	0.600	1500	(Guo and Suslick 2012)
Au/GR hydrogel	4-NP	Gel	14.6	0.190	31.7	(Li et al. 2012)
	MB		-	0.237	39.5	
CNFs@Au	4-NP	Core-shell Nanofiber	-	0.325	54.2	(Zhang et al. 2013)
GO@NH ₂ -Au NCs	4-NP	Nanosheets	14.0 \pm 1.0	2.136	2967	(Ju et al. 2014)
Fe@Au-GO	4-NP	Core-shell	10-12	0.121	-	(Gupta et al. 2014)
	2-NP			0.120	-	
Au/AC	<i>m</i> -dinitrobenzene	Nanowhisker	4	2.100	-	(Cárdenas-Lizana et al. 2015)
Au/MC-O	4-NP	Tube	10	0.465	0.1	(Guo et al. 2016)
Au/mSiO ₂ @RGO	4-NP	Two-Dimensional nanohybrid	3-5	0.900	37.5	(Maji and Jana 2017)
	MB			0.726	30.25	
Au/g-C ₃ N ₄	4-NP	-	2.6	0.479	7.99	(Fu et al. 2017)
Polydopamine-g-C₃N₄/Au	4-NP	-	25	3.084	10.28	(Qin et al. 2019)
Fe ₃ O ₄ @Carbon	4-NP	core-shell	15.9	5.34	89	(Gong et al. 2018)

1786

1787 **Table 5** Details of different parameters of Au-based multi-metal NPs for nitroaromatics

1788 reduction

Catalyst	Molar ratio	Structure	Recycles	Nitroaromatics	k_{app} (min ⁻¹)	k_{nor} (s ⁻¹ g ⁻¹)	Ref.
Ni@Au/SiO ₂	5:1	Core-shell dandelion	-	4-NP 2-nitroaniline	0.498 0.282	307 174	(Le et al. 2014)
PtAu alloy/CeO ₂	1:1	volcano	-	4-NP	6.522	2.174	(Zhang et al. 2014b)
Au-Ag/SiO ₂	6:1	nanorods	-	nitrobenzene	0.405	-	(Jayabal and Ramaraj 2014)
PCP@Au-Ag	1:1	Core-shell	6	4-NP	0.1722	144	(Fu et al. 2018)
Au-Pd/GO	4.53:1	flower	6	4-NP	-	-	(He et al. 2014)
PdAu/Fe ₃ O ₄	1:1	rod	8	4-NP	0.328	4.84	(Tuo et al. 2015)
Pt-Au/PDA@RGO	3:1	dendrimer	6	4-NP	0.575	1700	(Ye et al. 2016)
Fe ₃ O ₄ @TiO ₂ @Ag-Au	1:1	Core-shell	8	4-NP	0.115	3406.44	(Shen et al. 2017a)
Ni-Au/RGO	-	-	6	4-NP	0.662	36.77	(Li et al. 2017)
Au-Cu/RGO	3:1	-	-	4-NP	5.760	960	(Rout et al. 2017)
Pd/Au@g-C ₃ N ₄ -N	1:1	-	-	4-NP	0.791	52.72	(Fang et al. 2017)
Au@Pd@RuNPs	-	porous	6	4-NP Congo red Reactive red Reactive black	1.452 1.494 0.804 5.694	-	(Sahoo et al. 2015)

1789